UNCLASSIFIED

ATI 109 313

(U.S. MILITARY ORGANIZATIONS REQUEST COPIES FROM CADO. OTHERS ROUTE REQUESTS TO CADO THRU WADC W-P AFB DAYTON, OHIO, ATTN: WCNBA)

MC DONNELL AIRCRAFT CORP., ST. LOUIS, MO. (REPORT 2050)

GROUND TOW AND LOW ALTITUDE AUTOROTATION TEST RESULTS OF THE XH-20 HELICOPTER

GEORGE W. KALLAL 26 MARCH'51 66PP PHOTOS, TABLES, DIAGR, GRAPHS

USAF CONTR. NO. AF-33(038)-9845

HELICOPTERS - AUTOROTATION
HELICOPTERS - PERFORMANCE
H-20

ROTATING WING AIRCRAFT(34)
AERODYNAMICS AND PERFORMANCE (1)

UNCLASSIFIED

MAC 273 (REV. 2-24-50)

REPORT 2050

DATE 26 March 1951

REVISED

McDONNELL Aircraft Corporation

ST. LOUIS 3, MISSOURI

GROUND TOW AND LOW ALTITUDE AUTOROTATION TEST RESULTS OF THE XH-20 HELICOPTER

SUBMITTED UNDER Contract AF 33 (038)-9845

PREPARED BY George W. Kallal
George W. Kallal

APPROVED BY K. H. Hohenemser
K. H. Hohenemser

APPROVED BY Alan N. Heck
Alan N. Heck

APPROVED BY C. H. Hurkamp
C. H. Hurkamp

CONTENTS

1. SUMMARY

The McDonnell Aircraft Corporation presents the results of ground tow and low altitude autorotation tests for various configurations of the Model XH-20 helicopter in accordance with Item 2 of Contract AF 33 (038)-9845, P. R. 97219, E. O. No. 582-164 (SR-1). The report contains performance curves and data for simulated autorotative flight tests made by towing the rig-mounted helicopter on the ground in addition to performance curves for actual low altitude autorotative flights. The simulated autorotative flight performance data show the variation of rotor thrust coefficient with tip speed ratio and rotor angles from which are derived the rates of descent for the Model XH-20 helicopter. A comparison between the rates of descent as determined by the simulated autorotation tests and through theoretical calculations show that for low forward velocities and high rotor angles there is excellent agreement; and for high forward velocities and low rotor angles, a difference of only 7 per cent exists.

In addition to the preliminary or simulated flight tests, approximately 75 actual autorotative flights from altitudes below 320 feet are reported. They include a number of vertical descents from hovering at 60-70 feet. Due to the somewhat undesirable characteristics of the landing gear and the limited availability of the runways upon which to land,

spot landings without forward roll were necessary. This resulted in a variation of flight technique which frequently nullified any stabilizing RPM effect expected from the higher test altitudes. Despite the adverse flight restrictions, tests were performed satisfactorily and show conclusively that the relatively high rates of descent and steep glide angles associated with the present configuration result in no undue difficulty in flaring out and landing gently on a desired spot. The pilot suffered no discomfort during the high rates of descent after preliminary familiarization. Tests results, in addition to pilots' reports, indicate that a steady state rate of descent is closely approached at approximately 450 RPM with a blade pitch of one degree or at 400-420 RPM with a blade pitch of zero degrees. However, it was considered desirable to discontinue the autorotative flight tests because of inadequate landing gear which affected pilot technique, relatively low rotor speed which indicated small pull-up margins of safety, and resulting high stress level which adversely affected the fatigue life of the rotor. The speed of the rotor prior to flare-out decreased in most cases to approximately 30 RPM less than the RPM estimated to provide a desired margin of safety in the form of kinetic energy in case of pilot error.

2. INTRODUCTION

The McDonnell Aircraft Corporation presents the test results on the autorotation characteristics of the XH-20 helicopter in accordance with Item 2 of Contract AF 33 (038)-9845, P. R. 97219, E. O. No. 582-164 (SR-1).

A brief historical review of all preliminary autorotation tests and studies conducted by the contractor serves as a background for the more advanced autorotational data which is presented in this report. The history concerns the simulated autorotative flight tests made by mounting the flyable test stand on a truck and operating on a local highway, and by mounting the test stand behind the prop wash of a Navy JD-1 airplane. In addition to the tests are the studies that were made of pull-ups from power-off vertical descents and of the potential of helicopters to make safe autorotative descents.

The body of this report, however, concerns the more advanced testing of the XH-20 helicopter which is obtained by testing through two methods. In the first method, autorotative performance data is obtained without endangering the pilot nor subjecting the helicopter to possible damage through a series of simulated autorotative flight tests made on the ground in which the helicopter, mounted on a test rig, is towed by a truck on the airport runways. A second method, that for obtaining final results, is through a series of actual autorotative flights in which the helicopter makes power-off descents from altitudes.

In the simulated ground tow tests, three rotors of 20 foot diameter are tested to determine the effect of ram jet drag and the change in solidity on autorotation. The original data from these tests on which the performance data is based was reduced to a non-dimensional form and plotted as test points in Figures 6 through 9, 12 through 15, and 18 through 21, but was not included herein because of bulk. The performance data presented includes the relationship between rotor angles of attack, blade pitch, rotor tip speed ratio, rotor thrust coefficient, horizontal velocity and the rate of descent of the XH-20 helicopter. The resulting data is compared to the theoretical calculations of Reference 7.7 and an attempt is made to explain the reasons for the few discrepancies that were found to exist.

After ground tow tests and theoretical studies indicated that safe autorotative landings could be made with the 20 foot diameter rotor of .0531 solidity, a series of actual autorotative flights incorporating this rotor are made from low level altitudes with the XH-20 helicopter. To acquaint himself with the characteristics of the helicopter in autorotative flight, the pilot made power-off practice vertical descents from hovering at very low altitudes before proceeding with any autorotation flight with initial forward speed. After the period of familiarization, the pilot gradually increased altitude by increments unless a major change in the helicopter configuration compelled the process to be reestablished. The usual flight test technique is to attain a desired altitude and forward speed and then simultaneously turn off the fuel and decrease the collective pitch to a minimum to begin a power-off descent. Before contact with the ground, flare-out is initiated by an increase in collective pitch to the magnitude necessary to arrest the descent but not to cause ballooning. Throughout the flight regime, a motion picture camera focused on the photopanel records on film the fuel pressure, airspeed, altitude, rotor speed and collective pitch, the results of which are presented graphically in Figures 24-30 for seven representative actual autorotative flight tests.

3. HISTORY

Simulated autorotative flight tests at McDonnell Aircraft Corporation were conducted as early as July 1947, the results of which were promulgated in Reference 7.1. In the preliminary tests of the rotor alone, prior to the development of gasoline burning ram jets, the flyable test stand was mounted on a small pick-up truck and adjusted to a glide angle which resulted in the highest RPM for various airspeeds and pitch settings. Operations were conducted on a local four-lane highway. Results of the tests and preliminary calculations indicated that satisfactory autorotation was possible with a rotor employing ram jets.

After the development of suitable gasoline burning ram jets, a second series of autorotative tests were made employing the ram jets on the same 18 foot diameter rotor of 6.22 inch chord as used in the initial tests. In view of the high costs involved to obtain data through full scale wind tunnel tests, a much less expensive method was employed. Simulated wind tunnel tests were made utilizing the prop wash from a Navy JD-1 aircraft. The test stand was located approximately 120 feet behind the engine propellers. To simplify the supporting rig, the helicopter (flyable test stand) was blown at backward with the rudder removed as in Figure .1. With landing gear wheels removed, the front shocks were mounted on hinges to permit testing at various rotor angles. Two rotors of 18 foot diameter were tested; the first with a blade chord length of 6.22 inches and the second with a chord length of 8.22 inches. The second rotor was made after the tests of the first rotor indicated the need for a rotor of greater solidity. Results of both rotor tests are contained in Reference 7.9.

Meanwhile, autorotative landing studies were also performed using the work of D. L. L. Fitzwilliams (Reference 7.6) as a guide to the theoretical considerations which were limited to pull-ups from pure vertical descent through the use of only collective pitch control. The studies concerned the time increment available for a pull-up and the altitude from which a safe landing could be made by the use of the energy available, i.e., rotor kinetic energy. Two approaches were considered in these studies; the first was a rough approximation of the time and the altitude for a safe power-off descent from an initial hovering flight condition; the second was a calculation of the vertical descent characteristics and a reduction of the equilibrium vertical rate of descent by use of collective pitch control for the initial conditions of 50 feet per second rate of descent at 500 feet per second tip speed. Details of both methods appear in Reference 7.2.

Another study made was a comparison between autorotational landing potential of tip jet helicopters and conventional helicopters. An autorotational landing potential of a helicopter was expressed as the ratio of the kinetic energies available to arrest the steady state autorotation rate of descent to the kinetic energy of descent. The potential or capacity of the helicopter to make a safe autorotative landing increased with this ratio. The available energies that can be employed to arrest the steady state rate of descent are three in number; the usable kinetic energy of the rotor by collective pitch control, the kinetic energy of the horizontal component of the glide path velocity by cyclic pitch control, and the energy absorption capacity of the landing gear. Only the first two were considered in the determination of the landing potential of the helicopter and are discussed at length in Reference 7.3.

These preliminary tests and theoretical studies led to the selection of the test configurations employed in the ground tow tests, and serve as a background for the actual autorotative flight tests by the XH-20 helicopter. The results of both the simulated and actual autorotative flight tests are reported in the following pages.

4. NOTATIONS AND SYMBOLS

Ω	Rotor angular velocity, radians per second
R	Blade radius, feet
V	Resultant flight path velocity, feet per second
V_h	Horizontal component of flight velocity, feet per second
V_v	Rate of descent, feet per second
μ	Rotor tip speed ratio, $\frac{V \cos \alpha}{\Omega R}$
σ	Rotor solidity ratio, $\frac{b c}{\pi R}$
γ	Resultant glide angle
ρ	Air mass density, slugs per cubic foot
W	Gross weight, pounds
T	Rotor thrust
C_T	Rotor thrust coefficient, $\frac{T}{\rho \pi R^2 (\Omega R)^2}$
C_T/σ	Aerodynamic blade loading
C_{D_J}	Cold jet drag coefficient, $\frac{\text{jet drag}}{\rho/2 \, \pi R^2 (\Omega R)^2}$
$\left[\frac{D}{L}\right]$	Equivalent drag-lift ratio

$\left[\frac{D}{L}\right]_R$ Rotor equivalent drag-lift ratio $\left[\frac{D}{L}\right]_o + \left[\frac{D}{L}\right]_i$

$\left[\frac{D}{L}\right]_o$ Profile equivalent drag-lift ratio

$\left(\frac{D}{L}\right)_i$ Induced equivalent drag-lift ratio

$\left(\frac{D}{L}\right)_J$ Jet unit equivalent drag-lift ratio

$\left(\frac{D}{L}\right)_P$ Fuselage parasite equivalent drag-lift ratio

$\left(\frac{D}{L}\right)_G$ Glide or rate of descent equivalent drag-lift ratio

D Equivalent drag, pounds

α Angle of attack of plane perpendicular to control axis

f_s Fuselage flat plate area, $\left(C_D = 1.0\right)$, square feet

UNCLASSIFIED

ATI 109 313

(U.S. MILITARY ORGANIZATIONS REQUEST COPIES FROM CADO. OTHERS ROUTE REQUESTS TO CADO THRU WADC W-P AFB DAYTON, OHIO, ATTN: WCNBA)

MC DONNELL AIRCRAFT CORP., ST. LOUIS, MO. (REPORT 2050)

GROUND TOW AND LOW ALTITUDE AUTOROTATION TEST RESULTS OF THE XH-20 HELICOPTER

GEORGE W. KALLAL 26 MARCH'51 66PP PHOTOS, TABLES, DIAGR, GRAPHS

USAF CONTR. NO. AF-33(038)-9845

HELICOPTERS - AUTOROTATION
HELICOPTERS - PERFORMANCE
H-20

ROTATING WING AIRCRAFT(34)
AERODYNAMICS AND
PERFORMANCE (1)

UNCLASSIFIED

5. AUTOROTATIVE GROUND TOW TESTS

5.1 Apparatus And Instrumentation

A prerequisite of the simulated autorotative flight tests was that the helicopter operate at various attitudes of flight and at various flight velocities. Therefore, an apparatus consisting of a test rig was constructed to carry the helicopter at pre-selected attitudes of flight and a tow truck was used to provide the flight velocity. A photograph of the tow test equipment is presented in Figure 2.

Instrumentation consists of a Heiland 8" recording oscillograph which records blade pitch, rotor speed, towing air speed and thrust and drag forces. Both the anemometer and the oscillograph used to record towing speeds are mounted on the truck as in Figure 2. Rotor lift and drag forces are measured by means of strain gauge instrumentation - the strain gauges being mounted at the rotor hub as in Figure 3.

5.2 Test Configurations

A series of simulated autorotation flight tests employing three configurations are conducted to determine quantitatively the effect of ram jet drag and solidity on autorotative performance. All three configurations utilize a 20 foot diameter rotor and are the following:

(a) Rotor of .0435 solidity - no ram jets
(b) Rotor of .0435 solidity and ram jets
(c) Rotor of .0531 solidity and ram jets

5.3 Test Procedure

The test procedures employed with each of the three configurations are identical. However, prior to testing the rotor without ram jets, a weight of 3.70 pounds is fastened to each rotor blade tip to prevent the bending moment imposed on the blade from exceeding its maximum allowable value. A fairing is installed over the rotor tip weights to maintain drag values in accordance with the airfoil section for the blades. The test rig, with the helicopter at a pre-determined rotor angle, is then towed behind the truck to various pre-selected velocities until the rotor speed becomes constant, at which time the corresponding autorotational data is recorded. This procedure is repeated for other blade pitches and rotor angles.

The procedure for testing the rotor with ram jets is identical to that without ram jets except for large rotor angles. At large rotor angles, due to the weight of the ram jet engines, blade chordwise deflections result in excessive vibration at low rotor speeds. Consequently, it became necessary to attain a speed of approximately 650 RPM under ram jet power with the rotor in a horizontal plane before tilting to the desired rotor angle prior to towing. After the test rig is accelerated to the desired velocity, the fuel to the ram jet engines is shut off and rotor speed allowed to decrease to a constant RPM as governed by the forward velocity of the test rig. In all ground tow testing, the cyclic control stick is fixed in position after the rotor has passed through its critical vibration frequency. Rotor angles of attack selected for testing the rotor without ram jets are 23, 34, 44 and 48 degrees; and with ram jets, 23, 34, 44 and 53 degrees. Each rotor angle is tested with collective pitch settings of 0, ±2, and ±4 degrees. In plotting the results, a wide scatter of test points indicate that many tests for each blade pitch angle would be required before a mean value could be established.

5.4 Experimental Results

5.4.1 Data Analysis

A sample of the recorded data showing traces of magnitudes of thrust, drag, airspeed, collective pitch and rotor speed with their respective conversion factors obtained by calibration of the oscillograph appear in Figure 4. This original test data, being bulky in size, is omitted from the report but has been reduced to a nondimensional form, i.e., rotor thrust coefficient (C_T) and tip speed ratio (μ) for a given rotor angle and blade pitch angle. For tests of the rotor without ram jet engines, Figures 6, 7, 8 and 9 show the variation of the rotor thrust coefficient with tip speed ratio. Figures 12, 13, 14 and 15 give the variations for tests of rotors with ram jet engines while Figures 18, 19, 20 and 21 are for a rotor of higher solidity with the same ram jets.

For a helicopter (XH-20) of 550 pounds gross weight, values of thrust coefficient (C_T) are calculated for tip speeds of 350, 400, 450 and 500 feet per second and the corresponding autorotative values of tip speed ratio (μ) are obtained from the nondimensional test curves for various glide angles. Neglecting fuselage parasite drag, the horizontal and vertical components of simulated autorotative flight velocities are obtained as $V \cos \gamma$ and $V \sin \gamma$ respectively in accordance with Reference 7.7 and appear in Tables 1, 2, 3, 4, 5 and 6. The final plot of V_v vs V_h for each configuration is obtained by this procedure which may be summarized by the following steps:

(a) Assume a gross weight and range of tip speed (ΩR) and rotor angle α.

(b) Calculate rotor thrust coefficients for the above assumptions.

(c) For a given C_T and rotor angle α, read the tip speed ratio μ from the C_T vs μ graph.

(d) Knowing μ and ΩR and α, calculate V_v and V_h.

$$V_h = \mu \Omega R = V \cos \gamma$$

$$V_v = V_h \tan \alpha = V \sin \gamma$$

Figures 11, 17 and 23 present the results of the above steps as dimensional plots of the variation of rate of descent with horizontal velocity for various tip speeds. In addition, theoretical data is plotted on these graphs for comparative purposes. Results of this comparison are discussed in Section 5.5.

5.4.2 Experimental Test Results

There is considerable difference in the advance ratio range of the performance curves of thrust coefficient with tip speed ratio and rotor angle for the 20 foot diameter rotor, with and without ram jets. This difference is reflected in their respective rates of descent. As anticipated, the rotor without ram jets results in the lowest rate of descent of the three configurations tested - it having the lowest equivalent drag-lift ratio $\left(\frac{D}{L}\right)$ by virtue of no ram jet drag. However, the rotor of highest solidity, which should have given a lower rate of descent according to theory, actually resulted in rates of descent higher than the rotor of lower solidity - both rotors employing identical ram jets. This discrepancy may be explained by the increase in profile drag of the blade due to the manner by which the chord length was increased from 8.22 to 10.22 inches.

Test results show that incongruities exist in the rate of descent for a helicopter employing a rotor without ram jets flying with a forward speed of less than 27 ft/sec. and with a rotor tip speed of 350 ft/sec. Rates of descent with tip speeds in excess of 350 ft/sec. result in a congruent family of curves as in Figure 11.

A considerably higher rate of descent for a comparable horizontal velocity occurs with the addition of ram jet engines to the rotor. The corresponding rates of descent can be compared by inspecting Figures 11 and 17 which show that the test curves differ completely in that for a given rotor angle the curves inflect upward as in Figure 11 and deflect downward as in Figure 17.

For a ram jet operated rotor of increased solidity, the rate of descent for a given horizontal velocity is even greater, although contrary to the prediction by theory. In comparing Figures 17 and 23, it can be seen that at high horizontal velocities and at rotor angles of 23 degrees the curves differ in slope. With the high solidity rotor, Figure 23 indicates that no appreciable change in rate of descent occurs at a horizontal velocity in excess of 50 MPH, which is to be expected since the influence of fuselage parasite drag is excluded by the test method. For the rotor of decreased solidity, test results of Figure 17 indicate that an increase in horizontal velocity will result in a decrease in the rate of descent.

Since steady state rate of descent is only approached, and since no actual autorotative flights were made at a forward velocity greater than 30 MPH, no attempt was made to compare the results of ground tow tests with those of actual flight tests.

5.5 Test Data Comparison With Theory

5.5.1 Theoretical Analysis

The rate of descent of each of the three rotor configurations found experimentally can be evaluated by a comparison to the rate of descent calculated theoretically.

Therefore, the same gross weight of 550 pounds as used in determining the rotor thrust coefficient in the simulated autorotative flight tests is used in the theoretical calculations. The ram jet drag coefficient (C_{D_j}), based on rotor disc area, used in the analysis is .000122 which is representative of the ram jets used in the experimental tow tests. Values of drag-lift ratio for the ram jets $\left[\frac{D}{L}\right]_J$ are calculated from the equation given in Reference 7.7,

$$\left[\frac{D}{L}\right]_J = \frac{bD}{T}\left[\frac{1}{\mu} + \frac{3\mu}{2}\right].$$

Drag-lift ratio for the rotor $\left[\frac{D}{L}\right]_R$ for the various thrust coefficient-solidity ratios $\frac{C_T}{\sigma}$ are obtained from Reference 7.7. The two values are added as in Tables 2, 3 and 6 to obtain the theoretical rotor glide angle from which the rate of descent is determined. The equations used in brief are as follows:

$$\left[\frac{D}{L}\right]_G = \text{Tan } \gamma$$

$$\left[\frac{D}{L}\right]_G = \left[\frac{D}{L}\right]_o + \left[\frac{D}{L}\right]_i + \left[\frac{D}{L}\right]_p + b\left[\frac{D}{L}\right]_J$$

= Profile + Induced + Parasite + Jet

$$\text{Tan } \gamma = \left[\frac{D}{L}\right]_o + \frac{C_{T\ AUTO}}{2\mu^2} + \frac{f_s}{\pi R^2}\,\frac{\mu^2}{2C_{T\ AUTO}} + \frac{bD}{T}\left[\frac{1}{\mu} + \frac{3\mu}{2}\right]$$

As the fuselage parasite drag did not influence the rate of descent determined experimentally in that only forces on the rotor are measured, the parasite drag-lift ratio $\left(\frac{D}{L}\right)_p$ of the fuselage of the above equation is omitted in the theoretical calculations.

5.5.2 Comparison of Test Results With Theory

The variation of rate of descent with horizontal velocity and tip speed from simulated autorotative flight tests of a 20 foot diameter rotor without ram jets is plotted and compared, in Figure 11, to results obtained from theory. The two curves compare excellently particularly at low forward velocities for all tip speeds and at high rotor angles, if the extended theoretical curves as indicated by the dotted lines are assumed as being correct. At horizontal velocities above approximately 35 MPH, theoretical calculations are optimistic compared with test results indicating that the profile drag for the test rotor blade is greater than average. The identical rotor, to which ram jets are added, produces a more harmonious agreement between test and theory, as seen in Figure 17, where the maximum difference between them is 7 per cent for any rotor speed at 40 MPH forward velocity. The discrepancies that exist between test and theoretical rates of descent at low rotor angles and comparatively high forward speeds can be justified on the basis of ground effect, instrument error, erroneous assumptions as to profile drag coefficient and data analysis. From Figure 6 it is evident that at a rotor angle of approximately 23 degrees, the mean height of the rotor disc is only .70 rotor diameter above the ground which is within the range of ground effect.

Autorotative performance test data for the ram jet operated rotor of .0531 solidity is obtained by the same methods as in the previous two series of tests. Results with this rotor are similar to those of the other two configurations except that excellent agreement between test results and theoretical calculations are obtained for rates of descent at tip speeds below 500 ft/sec. and rotor angles of 34 degrees and above. At 50 MPH forward velocity, maximum discrepancy between test results and theory is 7 per cent and that occurring at 500 RPM rotor speed. The discrepancy can be attributed to the poorly constructed rotor blades resulting in high profile drags at high tip speeds.

An increase in rotor solidity from .0435 to .0531 (chord length 8.22 to 10.00 inches) result in little change in rate of descent at rotor tip speeds below 450 ft/sec. and rotor angles greater than 34 degrees. From an aerodynamic standpoint, the rework of the blade to 10.00 inches is considered unsatisfactory. Correct solidity is obtained but at the expense of cleanliness of design. For reasons of economy, the rotor with blade chord length of 8.22 inches was increased to 10.00 inches simply by riveting an extension to the trailing edge. At that time, it was believed that, although the contour of the blade left much to be desired, the effect on autorotation by the reworked blade would be within the accuracy of the ground tow tests.

6. LOW ALTITUDE AUTOROTATIVE FLIGHT TESTS

6.1 Apparatus And Instrumentation

After preliminary ground tow tests and theoretical studies indicated that safe autorotative landings could be made with the 20 foot diameter rotor, it was decided to perform and record a series of actual autorotative flights from low altitudes. In addition to the normal instrumentation carried by the helicopter, consisting of an altimeter, tachometer, airspeed indicator and fuel pressure gauge, two sliding indicators (one to measure collective pitch angles and the other to indicate cyclic pitch position with respect to the fuselage) were added as in Figure 5. In order to record the necessary data, a motion picture camera focused on the instrument panel is mounted above the head of the pilot. A switch, located on the cyclic control stick and operated by the pilot, controls the operation of the camera. Both the camera and instrument panel were rigidly mounted to the helicopter frame after several flight tests indicated the need for eliminating excessive vibration. Except for lag and natural frequency of oscillation within the tachometer, the instrumentation is considered satisfactory.

Rotor configuration (C) of Section 5.2, identical to that used in ground tow tests, is employed for all actual autorotative flights.

6.2 Test Procedure

To familiarize himself with the characteristics of the helicopter in autorotative pull-ups, the pilot made practice power-off, vertical descents from hovering from approximately 60-70 feet altitude with the XH-20 helicopter before undertaking any autorotative flight with initial forward speed. After the period of familiarization, the pilot increased altitude by increments of approximately 20 feet, unless a major change in the helicopter configuration compelled the process to be reestablished.

The usual autorotation flight technique employed in testing the XH-20 helicopter is the following. After attaining sufficient rotational speed for hovering, the pilot takes off, ascends to the desired altitude and flies with a forward velocity of approximately 25 MPH. Having approximately 650 RPM rotor speed and approximately 5 degrees collective pitch, the fuel to the ram jets is shut off. Immediately after the fuel pressure drops to zero pressure, indicating that the ram jets are inoperative, the collective blade pitch is decreased to a minimum and the rotor allowed to decelerate in power-off descent. According to the traces, flare-out is initiated at approximately 50 feet above the ground when collective pitch is increased rapidly to a degree which halts the vertical descent, but at the same time does not cause the helicopter to balloon. The pilot maintains, however, that he began flare-out at approximately one-half the indicated height.

6.3 Experimental Results

6.3.1 Data Analysis

Experimental results of autorotative flight tests of the Model XH-20 helicopter appear in Figures 24 through 30 inclusive on which are plotted a variation of RPM, collective blade pitch, altitude, fuel pressure and indicated airspeed (obtained from photo panel data) with respect to time measured in camera frames. As the time required for the autorotative flights is of short duration and almost impossible to read accurately on the clock, the camera frames are counted, and, knowing the camera speed, the elapsed time is easily determined. Every twentieth frame is read and plotted. Autorotation, as noted in Figures 24-30, lies between zero fuel pressure and the point at which the collective blade pitch is increased from its minimum value.

It is of interest to note from the same figures that when entering into autorotation, the direction of airflow through the rotor changes from downward to upward resulting in a change in pressure beneath the rotor that causes a recorded erroneous increase of altitude of approximately 20 to 40 feet. For a more accurate altitude curve these points were ignored. Figure 25 indicates that the altimeter is affected by inertia forces and/or ground effect inasmuch as sub-ground level altitudes are recorded. With the influence of ground effect, setting the altimeter to indicate correct altitudes under all phases of flight becomes almost an impossibility.

Assuming that the instruments are read accurately from the camera film, the tachometer, altimeter and airspeed indicator each have an inherent frequency of oscillation as denoted by the test points in Figures 24-30. However, the curves are constructed through the mean test points and represents the actual condition that exists.

It is apparent from the curves that the instrument most affected by sudden changes in flight or vibration and most erratic in amplitudes of oscillation is the magnetic tachometer which replaced the unsatisfactory chronometric tachometer. Despite its shortcomings, performance of the magnetic tachometer is considered satisfactory.

6.4 Discussion

Of the 75 autorotative power-off descents performed, some of which were discussed in References 7.4 and 7.5, seven flights considered most representative are plotted in Figures 24-30 inclusive. They show a rate of descent ranging from 30 ft/sec. to 48 ft/sec., the former with 1 degree collective pitch setting during autorotation and the latter with 0 degrees collective pitch. To obtain the design maximum of 11 degrees collective pitch for flare-out and pull-up, more autorotative flights are made with collective pitch at 1 degree than with 0 degrees. However, as the rotor speed appears to be approaching stabilization at approximately 450 RPM, with more than sufficient energy remaining for flare-out, the collective pitch angle is reduced from 1 degree to 0 degrees.

A comparison of Figures 29 and 30 with 24-28 will demonstrate that the slope of the RPM curve for zero degrees collective pitch is not as steep as with one degree, prior to flare-out. With zero degrees collective pitch in autorotation, stabilization appears to occur at approximately 400-420 RPM. However, prior to flight testing, 450 RPM was estimated as the minimum rotor speed necessary for flare-out and to provide a margin of safety in the advent of pilot error For lack of more concrete knowledge, therefore, a rotor speed of 400-420 RPM must be considered marginal. In all 75 autorotative flights, however, not one descent was made in which the landing gear was forced to cushion the landing. Due to the somewhat undesirable characteristics of the landing gear, the autorotative landings were to be made without any appreciable forward roll. Combined with limited runways upon which to land unless the wind direction paralleled the runways, a variation of flight technique was required so that in many cases when descents were made from the higher altitudes tested, collective pitch was also applied at a higher altitude, resulting in a rotor deceleration period of the same length as those of the lower altitude flights.

The inadequate landing gear which affected pilot technique, the relatively low rotor speed which indicated small pull-up margins of safety, and the lack of knowledge as to the stress level in the blades during these tests made further autorotative flight testing undesirable with the present configuration. Excluding the ram jet, to improve the autorotative characteristics, the following three modifications are recommended; the rotor blades be constructed to a known and desired contour for low profile drag, the fuselage be redesigned for low parasite drag, and the landing gear be made more suitable for ground maneuvers. These modifications, when incorporated, should result in a satisfactory configuration for autorotation.

7. REFERENCES

7.1 Ballauer, A. C., Progress Report 11, Ram Jet Helicopter Rotor Development. 15 August 1947.

7.2 Ballauer, A. C., Progress Report 33, Ram Jet Helicopter Rotor Development. MAC Engineering Report 1273, 15 June 1949.

7.3 Ballauer, A. C., Progress Report 41, Ram Jet Helicopter Rotor Development. MAC Engineering Report 1572, 15 February 1950.

7.4 Ballauer, A. C., Progress Report 46, Ram Jet Helicopter Rotor Development. MAC Engineering Report 1764, 15 July 1950.

7.5 Ballauer, A. C., Progress Report 47, Ram Jet Helicopter Rotor Development. MAC Engineering Report 1793, 15 August 1950.

7.6 Fitzwilliams, D. L. L., "Engine-Off Landings", Flight Magazine, 13 November 1947.

7.7 Heck, Alan, Charts For Estimating The Autorotative Performance Of Jet Rotors. MAC Engineering Report 1079, 18 March 1949.

7.8 Heck, Alan, Effect of Design Parameter Variation On Autorotation And Hovering Performance Of Jet Rotor Helicopters. MAC Report 1691, 15 May 1950.

7.9 Toney, E., Progress Report 29, Ram Jet Helicopter Rotor Development. MAC Engineering Report 1081, 14 February 1949.

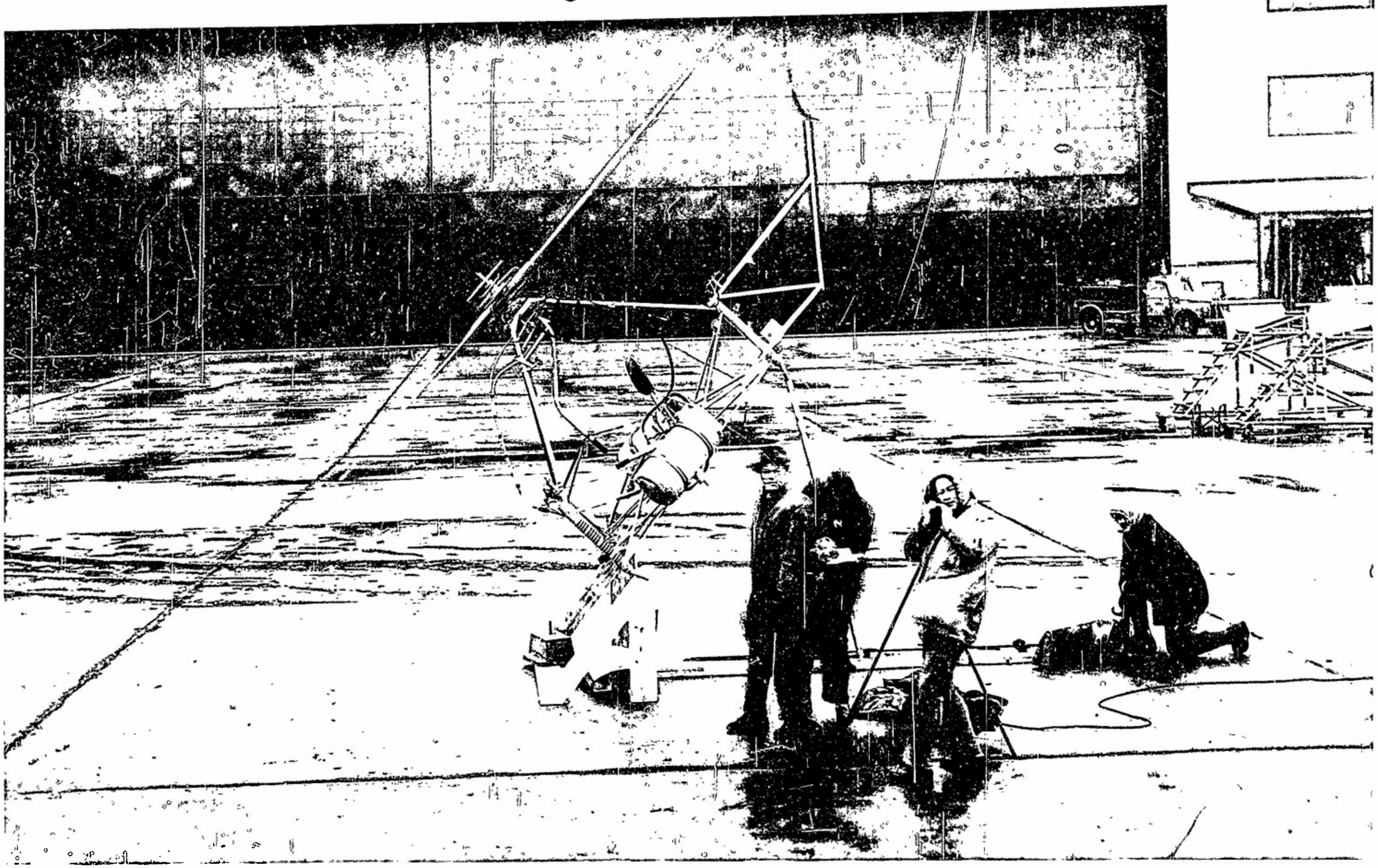

Figure 1
D4H-12312

HELICOPTER IN PROP WASH OF NAVY JD-1

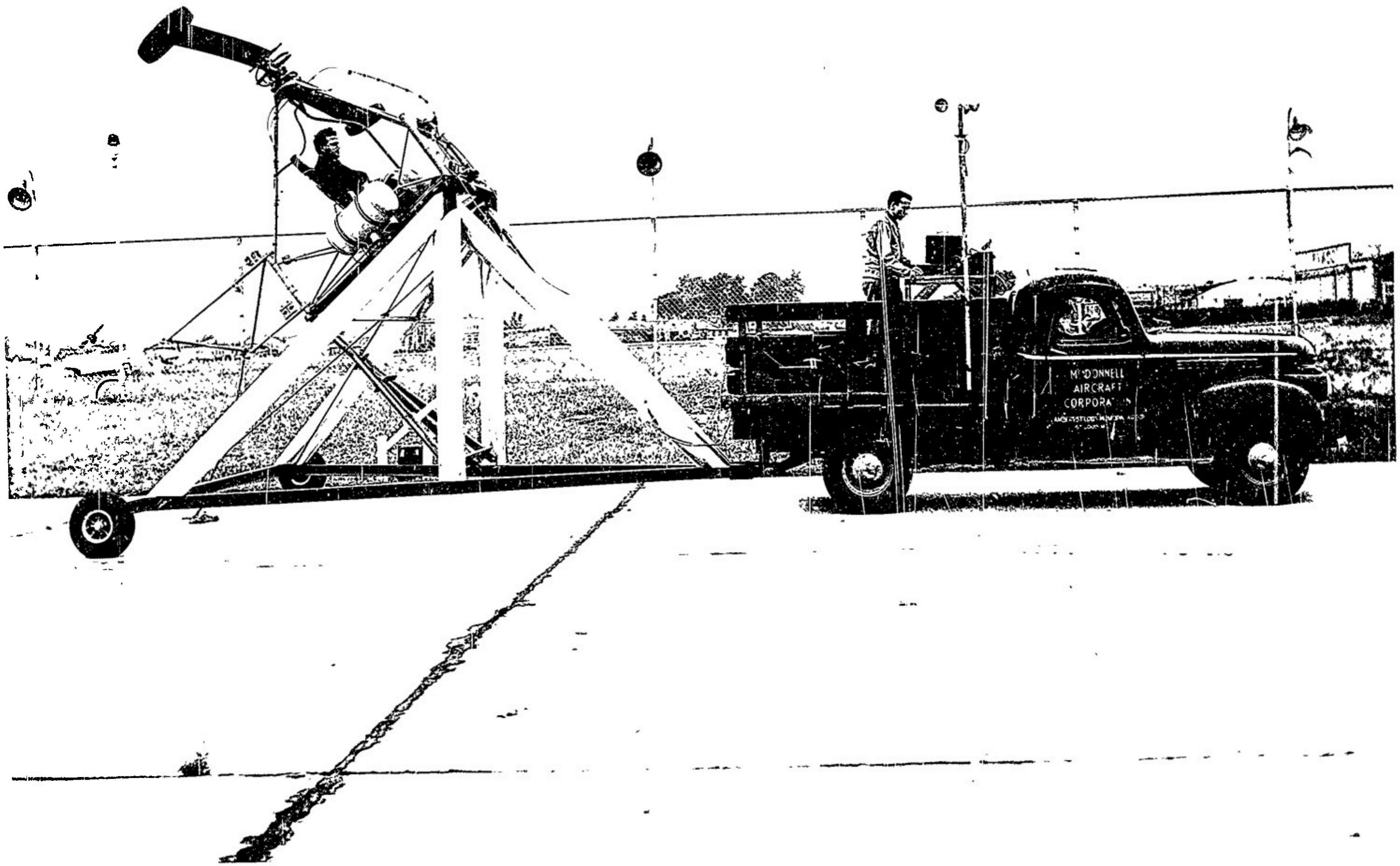

Figure 2
D4H-15179

FLYABLE TEST STAND MOUNTED IN RIG
WITH TRUCK IN TOWING POSITION

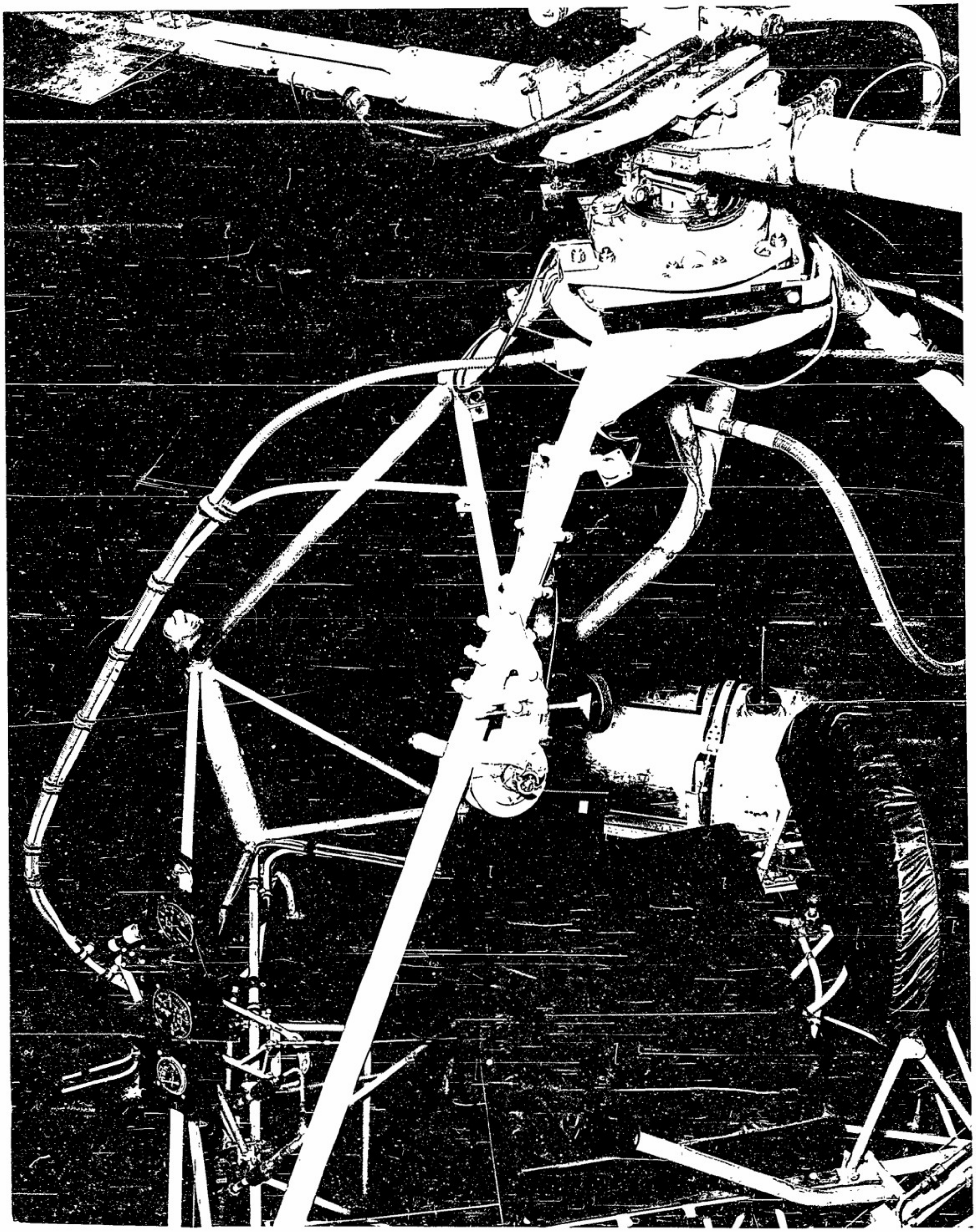

Figure 3 FLYABLE TEST STAND STRAIN GAUGE INSTRUMENTATION Report 2050
D4H-14765

TYPICAL TRACE FOR AUTOROTATION DATA FOR 20 FT. DIA. ROTOR WITH NO. 26 AND 27 JETS AT APPROXIMATELY 45° ROTOR ANGLE OF ATTACK.

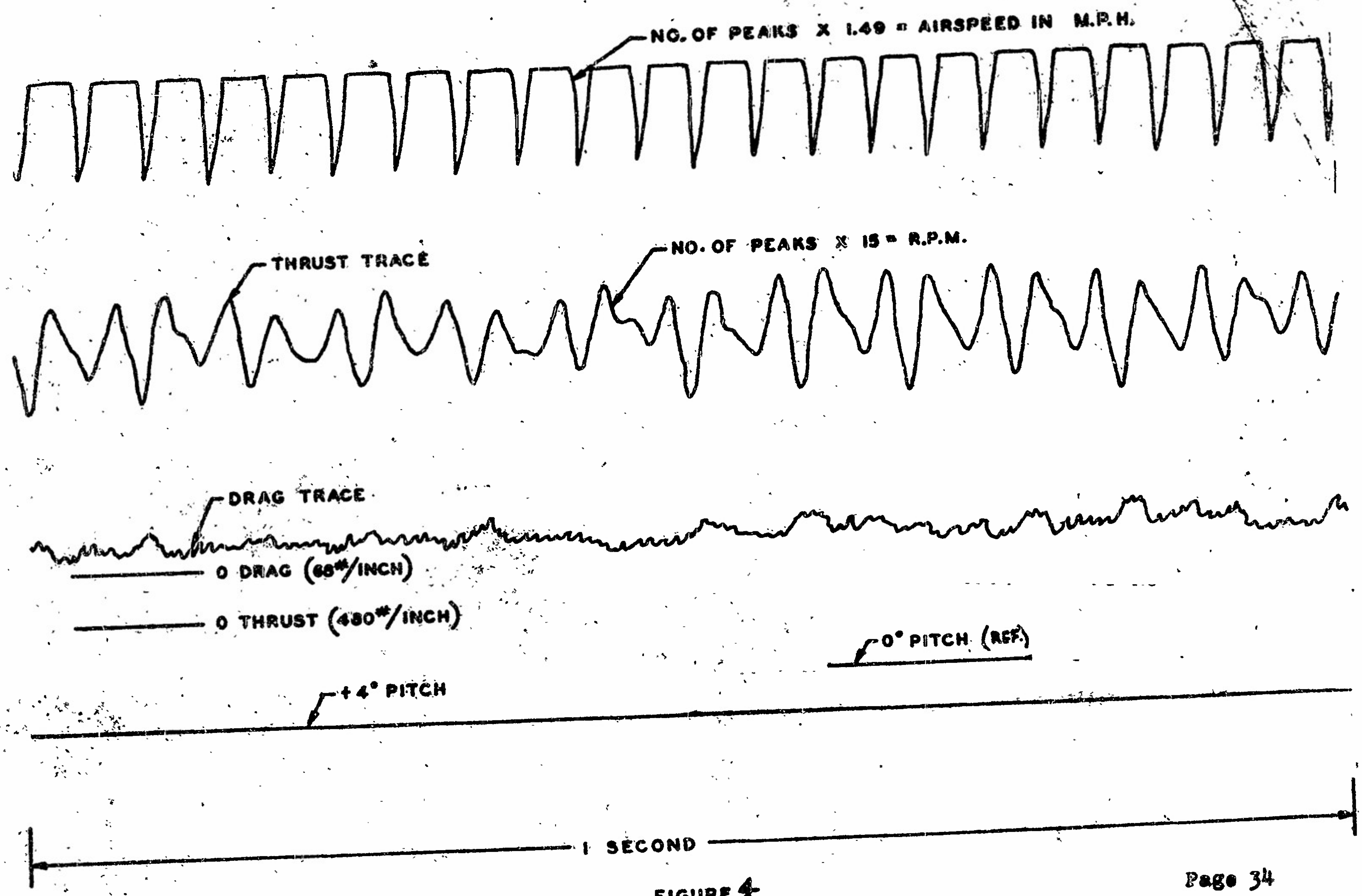

FIGURE 4

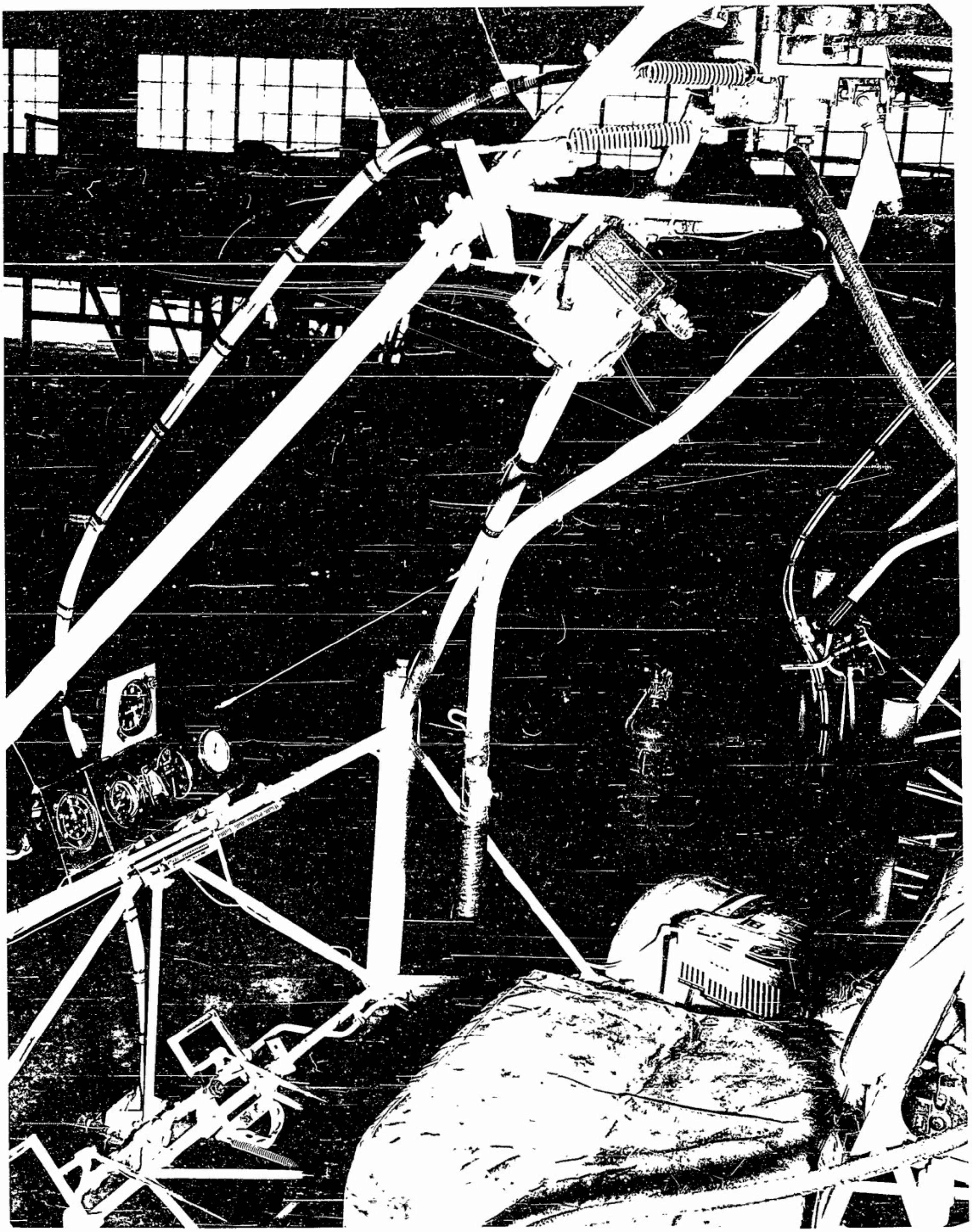

Figure 5 CAMERA INSTALLATION FOR
D4H-14326 LOW ALTITUDE AUTOROTATION FLIGHT TESTS Report 2050

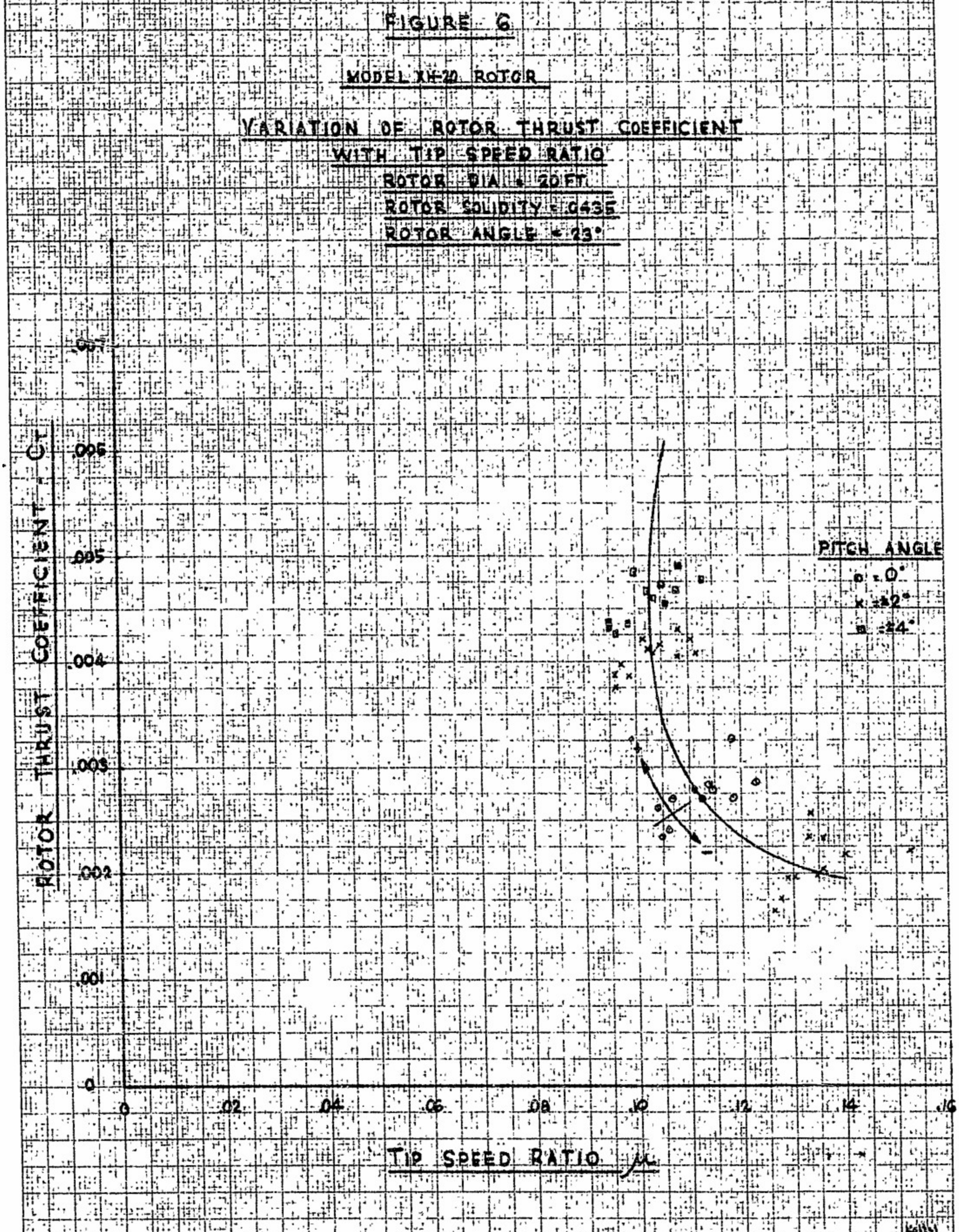
FIGURE 6
MODEL XH-20 ROTOR
VARIATION OF ROTOR THRUST COEFFICIENT
WITH TIP SPEED RATIO
ROTOR DIA = 20 FT.
ROTOR SOLIDITY = .0435
ROTOR ANGLE = 23°
ROTOR THRUST COEFFICIENT - CT
.006
.005
.004
.003
.002
.001
0
0
.02
.04
.06
.08
.10
.12
.14
.16
TIP SPEED RATIO μ
PITCH ANGLE
⊙ = 0°
x = 2°
▣ = 4°

FIGURE 7

MODEL XH-20 ROTOR

VARIATION OF ROTOR THRUST COEFFICIENT WITH TIP SPEED RATIO

ROTOR DIA. = 20 FT.

ROTOR SOLIDITY = .0435

ROTOR ANGLE = 34°

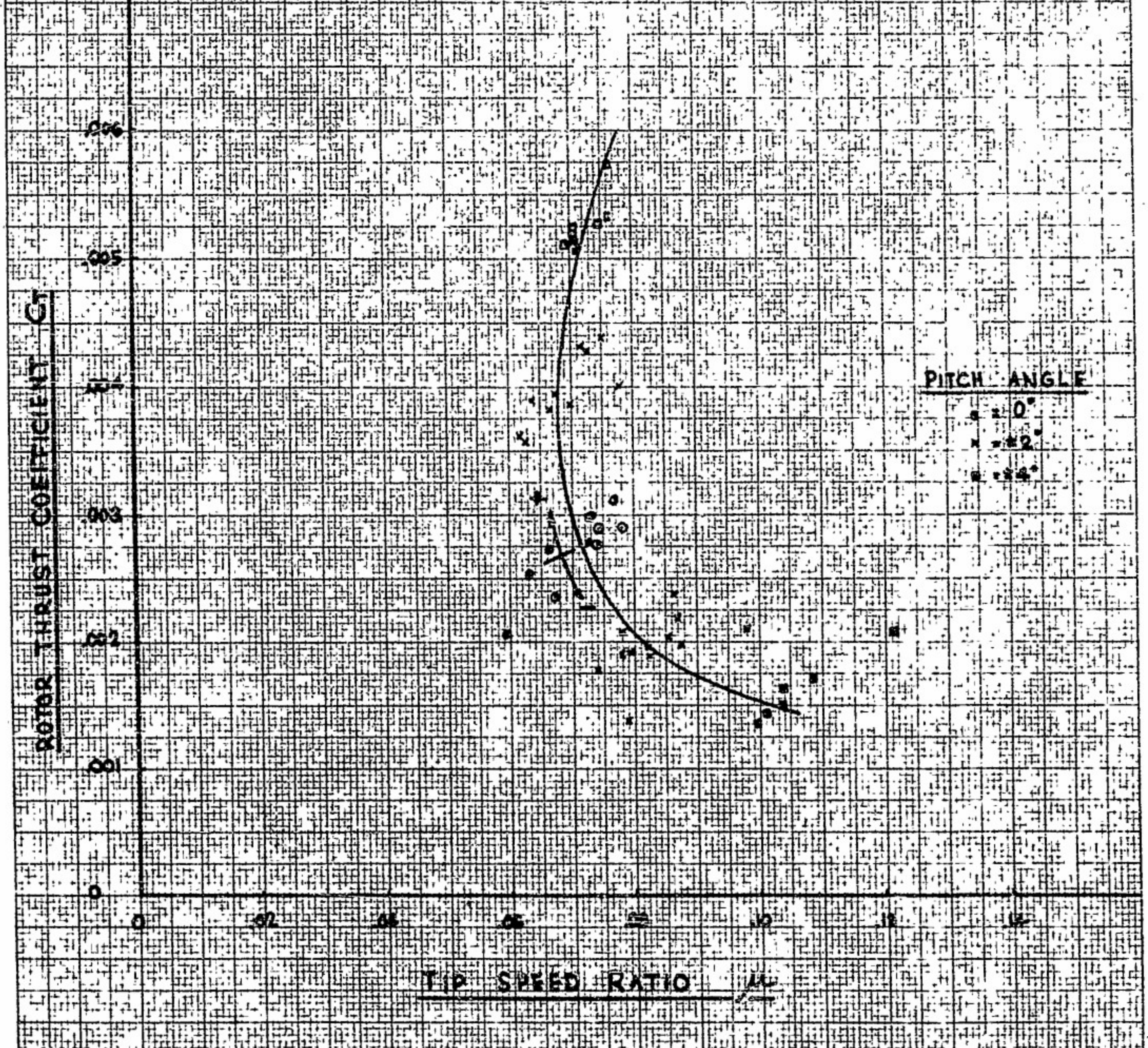

FIGURE 8

MODEL XR-20 ROTOR

VARIATION OF ROTOR THRUST COEFFICIENT
WITH TIP SPEED RATIO
ROTOR DIA. = 20 FT.
ROTOR SOLIDITY = .0435
ROTOR ANGLE = 4°

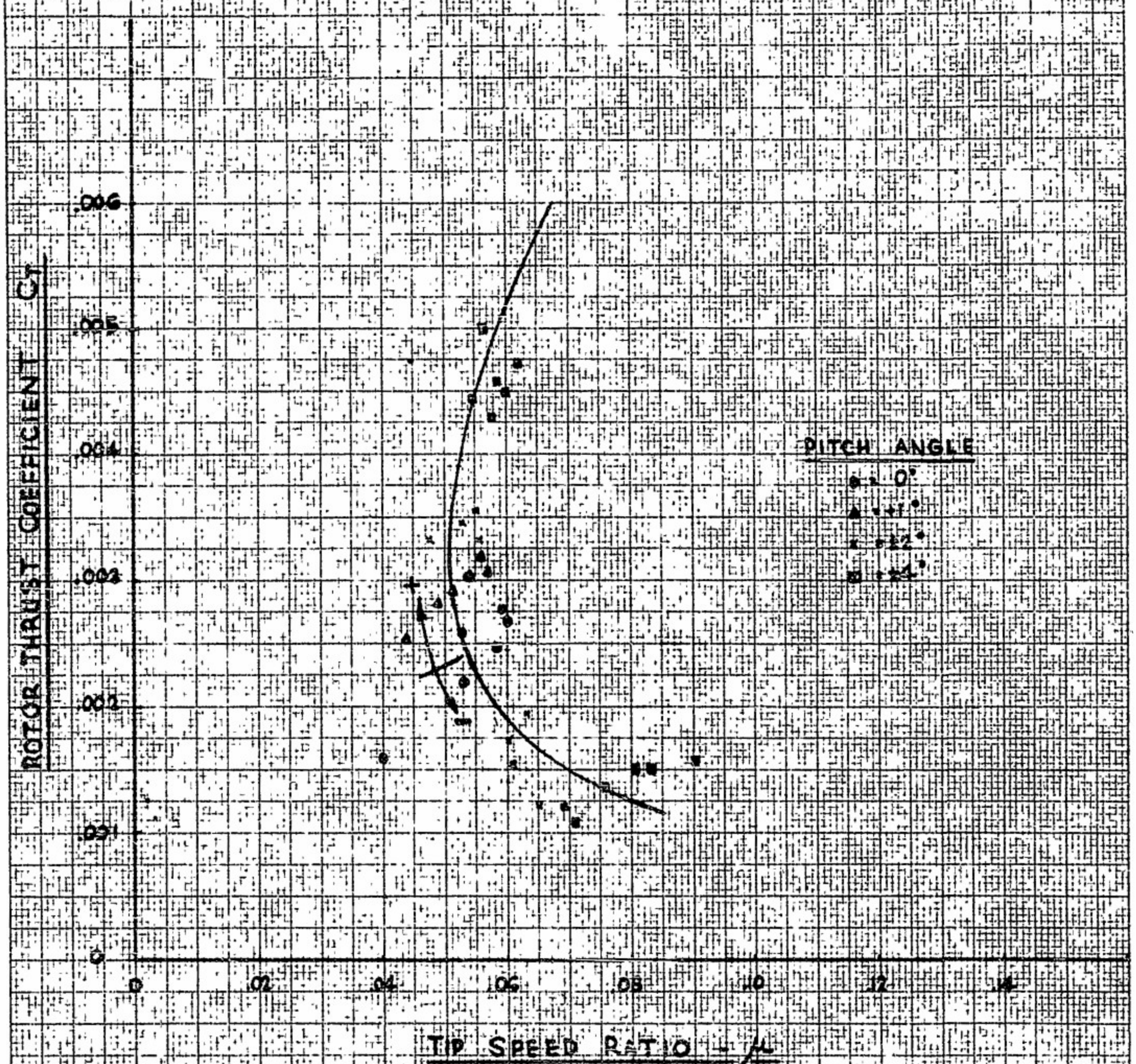

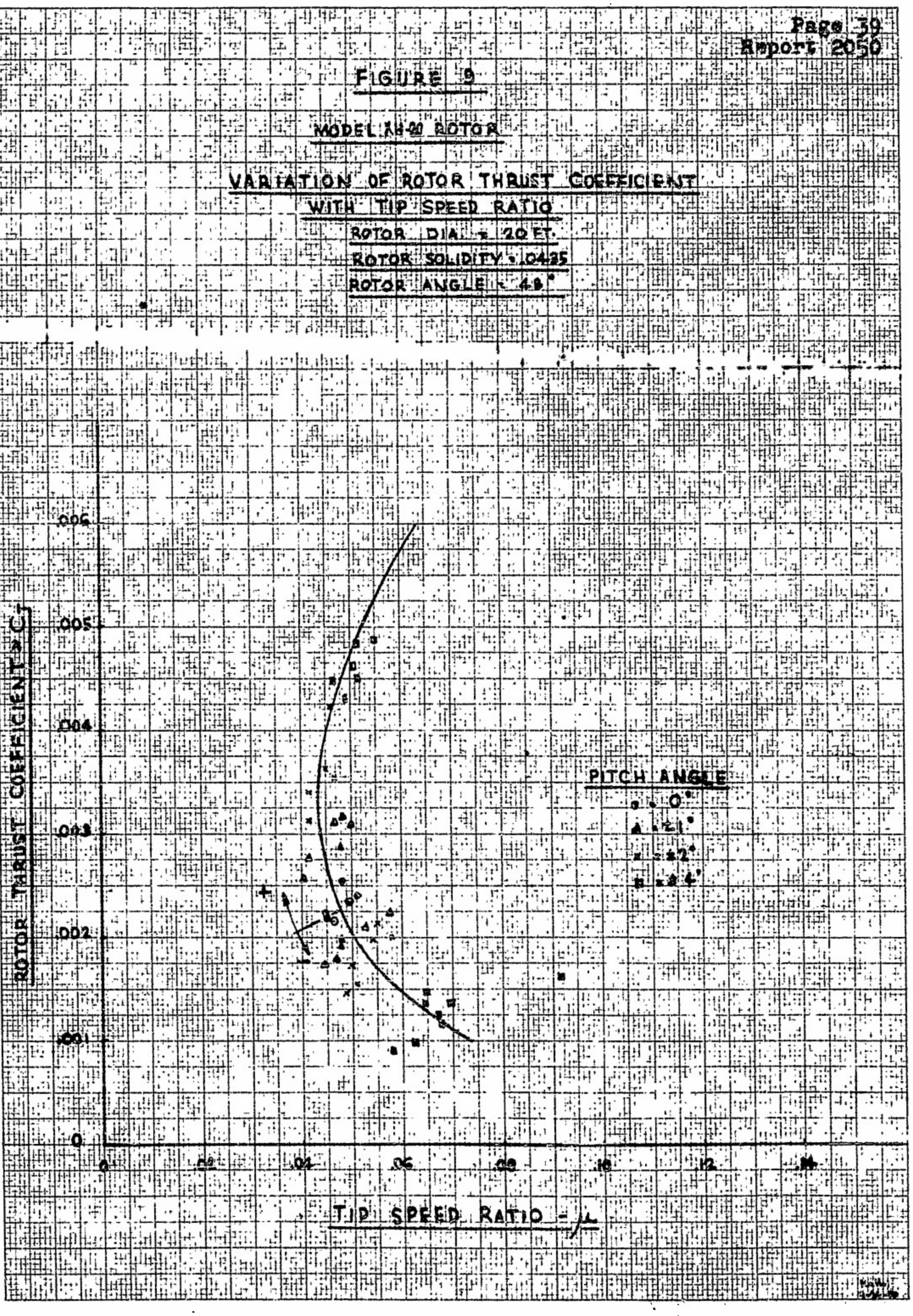
FIGURE 9
MODEL AH-20 ROTOR
VARIATION OF ROTOR THRUST COEFFICIENT
WITH TIP SPEED RATIO
ROTOR DIA. = 20 FT.
ROTOR SOLIDITY = .0435
ROTOR ANGLE = 43°
ROTOR THRUST COEFFICIENT - C_T
.006
.005
.004
.003
.002
.001
0
.02
.04
.06
.08
.10
.12
.14
TIP SPEED RATIO - μ
PITCH ANGLE
0°
2°
4°

FIGURE 20

MODEL XH-20 ROTOR

VARIATION OF ROTOR THRUST COEFFICIENT WITH TIP SPEED RATIO AND ROTOR ANGLE

ROTOR DIA. = 20 FT.

ROTOR SOLIDITY = .0435

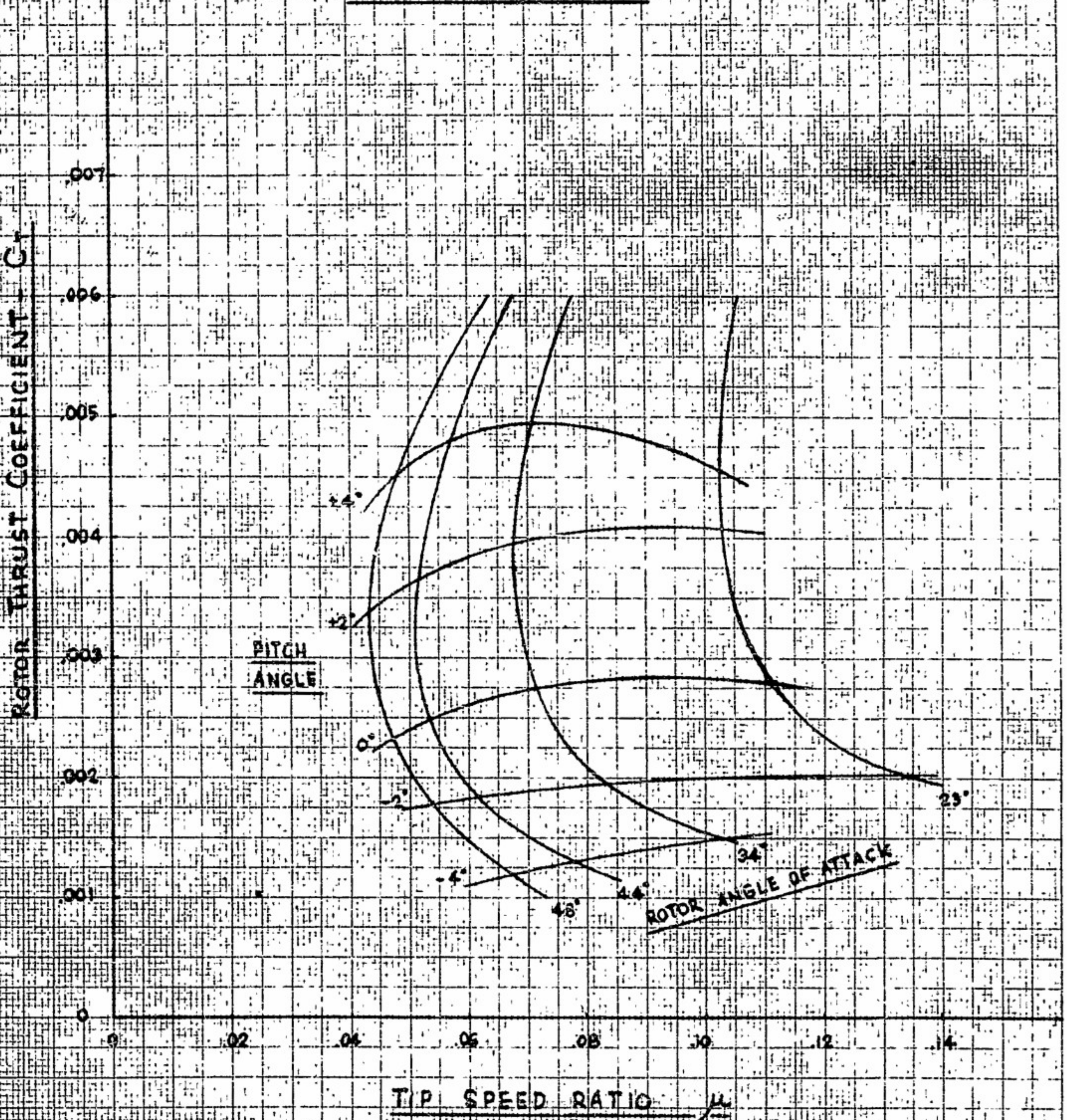

TABLE 1

Test Dimensional Plot for Rate of Descent

Gross Weight = 550 pounds

Rotor Diameter = 20 feet

Rotor Solidity = .0435

		TEST			
γ	ΩR	350	400	450	500
	C_T	.00601	.00461	.00364	.00295
23°	μ	.106	.1025	.104	.1092
	V_h	37.8	41.0	46.6	54.6
	V_v	16.0	17.4	19.8	23.2
34°	μ	.0775	.069	.0675	.070
	V_h	27.15	27.6	30.4	35.0
	V_v	18.3	18.6	20.5	23.6
44°	μ	.0675	.056	.0515	.051
	V_h	23.6	22.4	23.2	25.5
	V_v	22.8	21.6	22.6	24.6
48°	μ	.0635	.0488	.0438	.044
	V_h	22.23	19.5	19.7	22.0
	V_v	24.6	21.6	22.0	24.4

TABLE 2

Theoretical Dimensional Plot for Rate of Descent

Gross Weight	550 pounds
Rotor Diameter	20 feet
Rotor Solidity	.0435

Theory					
μ	ΩR	350	400	450	500
.10	$\left[\frac{D}{L}\right]_R = \tan\gamma$	.438	.369	.338	.323
	V_h	35.0	40.0	45.0	50.
	V_v	15.33	14.76	15.21	16.15
.15	$\left[\frac{D}{L}\right]_R = \tan\gamma$	.229	.198	.188	.188
	V_h	52.50	60.0	67.5	75.0
	V_v	12.02	11.88	12.69	14.20
.20	$\left[\frac{D}{L}\right]_R = \tan\gamma$	.151	.135	.130	.135
	V_h	70.0	80.0	90.0	100.0
	V_v	10.57	10.80	11.70	13.50
.25	$\left[\frac{D}{L}\right]_R = \tan\gamma$	.111	.103	.101	.105
	V_h	87.50	100.0	112.5	125.0
	V_v	9.71	10.30	11.36	13.12

FIGURE 11

MODEL XH-20 ROTOR

VARIATION OF RATE OF DESCENT WITH HORIZONTAL VELOCITY AND TIP SPEED

ROTOR DIA. = 20 FT.

ROTOR SOLIDITY = .0435

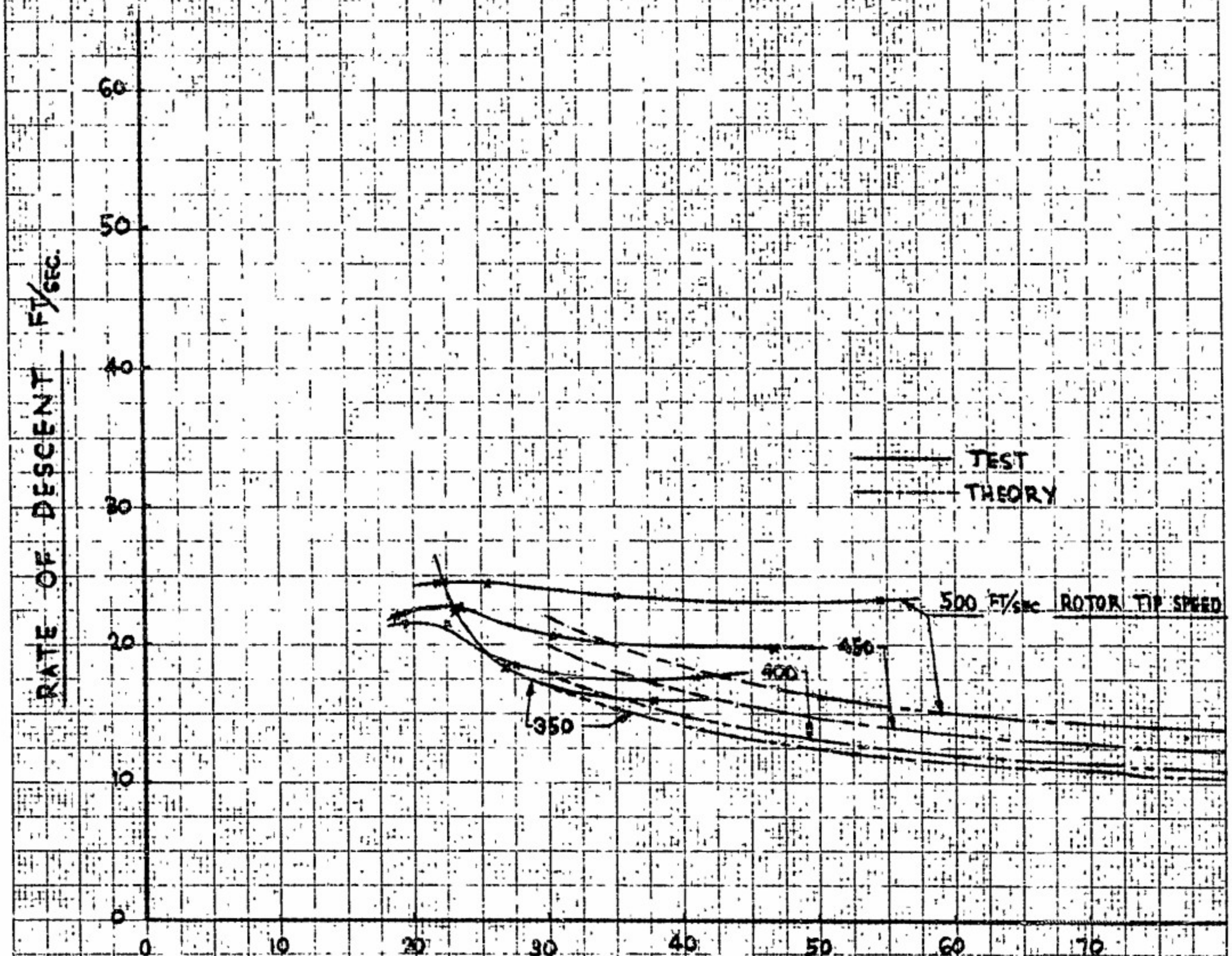

FIGURE 12

MODEL X[illegible] ROTOR AND RAMJETS

VARIATION OF ROTOR THRUST COEFFICIENT
WITH TIP SPEED RATIO FOR
ROTOR DIA. = 20 FT.
ROTOR SOLIDITY = .0435
RAMJETS # 26 & # 27 (MOD. EXIT # 2)
ROTOR ANGLE = 23°

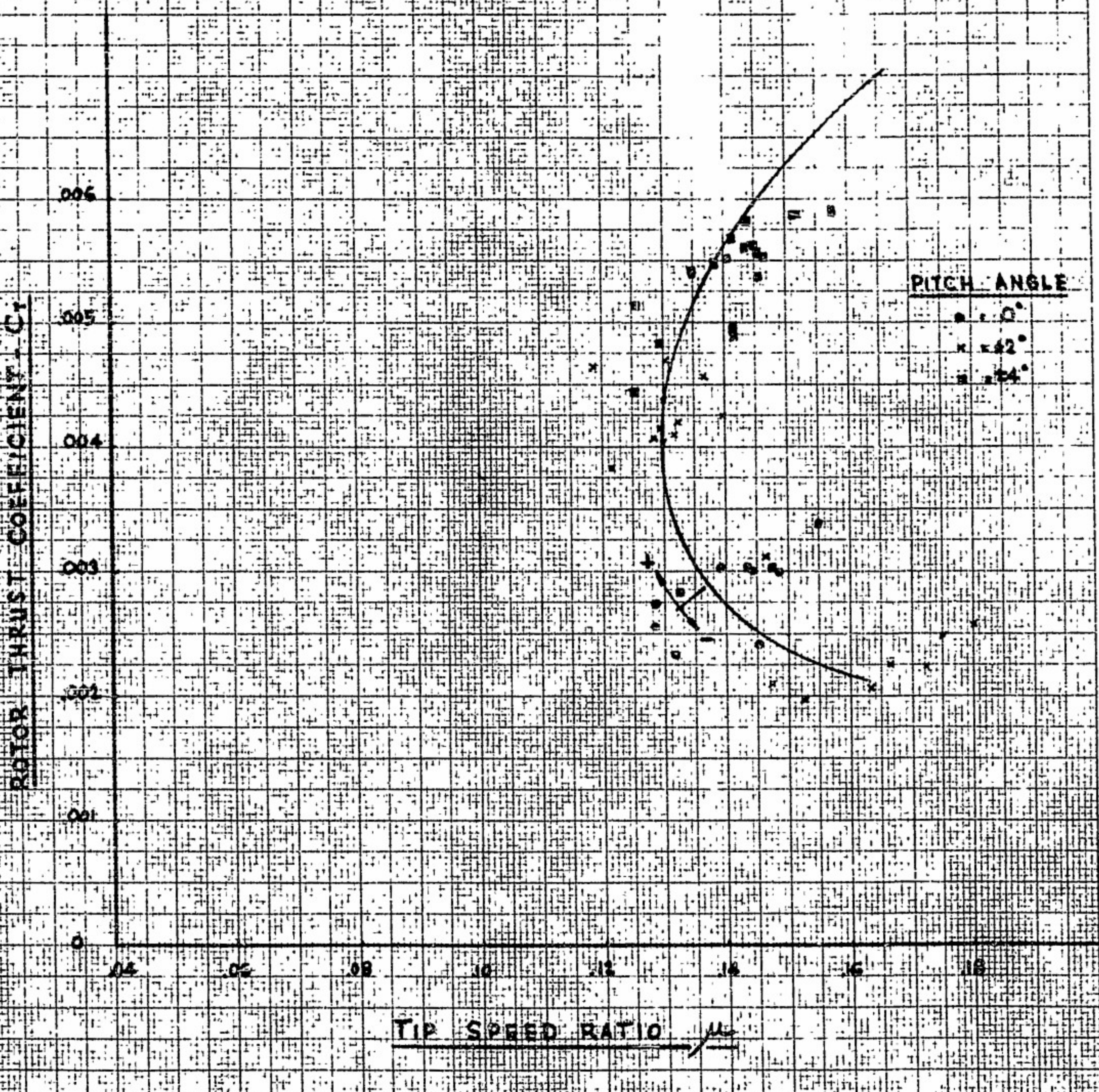

FIGURE 13

MODEL [illegible] ROTOR AND RAMJETS

VARIATION OF ROTOR THRUST COEFFICIENT
WITH TIP SPEED RATIO FOR

ROTOR DIA. = 20 FT.
ROTOR SOLIDITY = .0435
RAMJETS #26 & 27 [MOD. EXIT #2]
ROTOR ANGLE = 34°

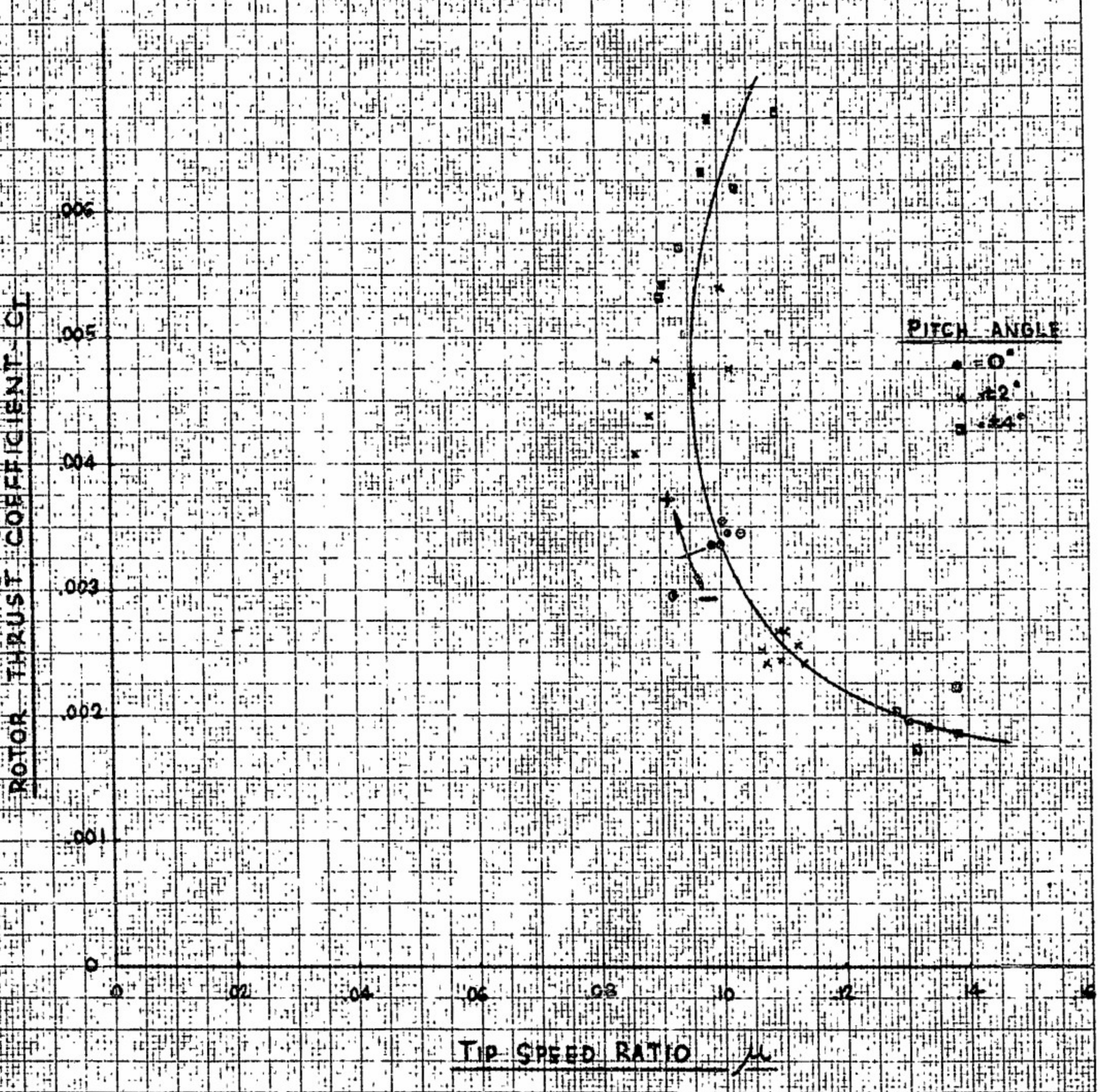

FIGURE 14

MODEL XR-2? ROTOR AND RAMJETS

VARIATION OF ROTOR THRUST COEFFICIENT
WITH TIP SPEED RATIO FOR
ROTOR DIA. = 20 FT.
ROTOR SOLIDITY = .0435
RAMJETS #26 & #27 [MOD. EXIT #2]
ROTOR ANGLE = 4°

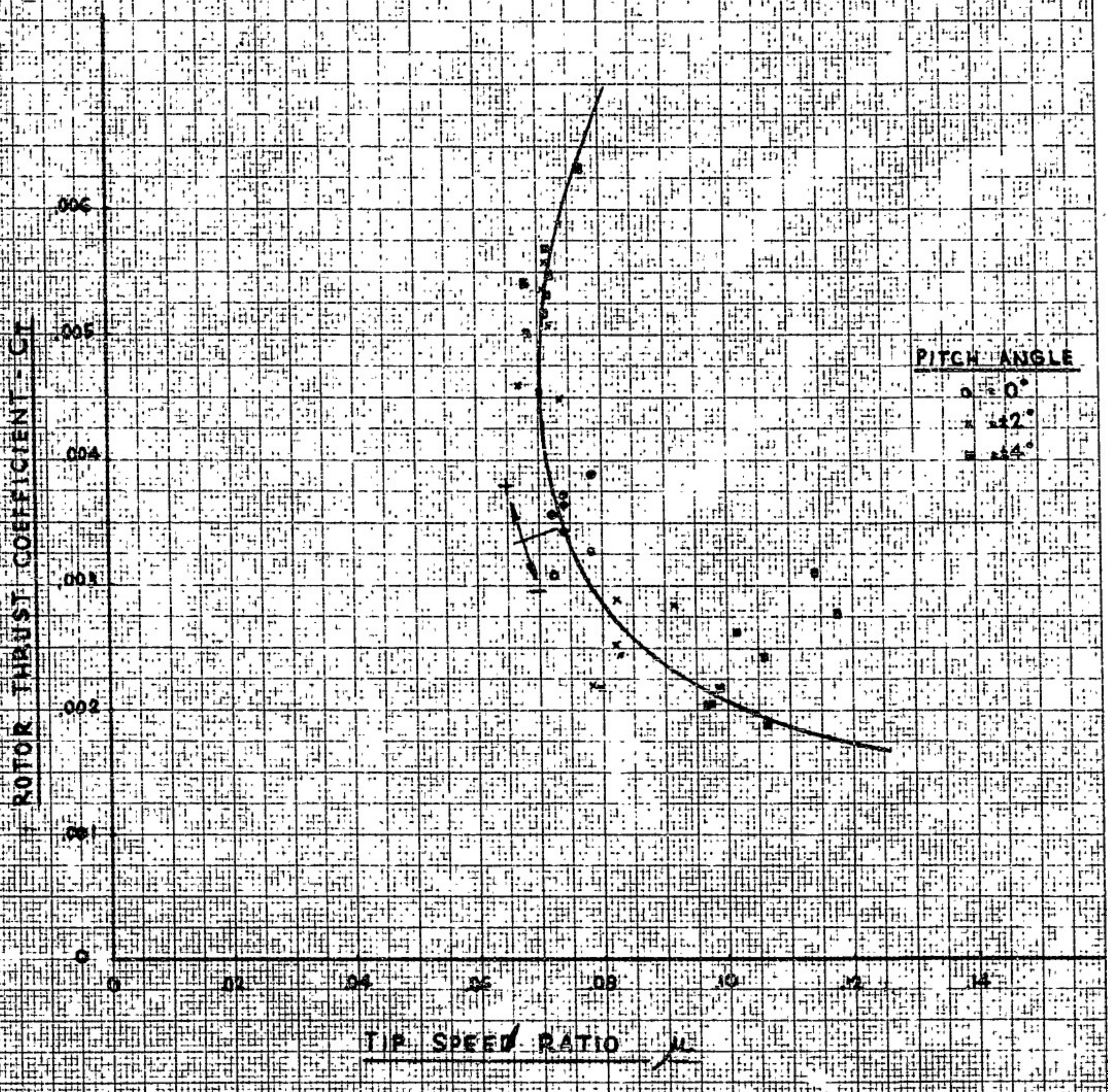

FIGURE 15

MODEL XH-20 ROTOR AND RAMJETS

VARIATION OF ROTOR THRUST COEFFICIENT
WITH TIP SPEED RATIO FOR
ROTOR DIA. = 20 FT.
ROTOR SOLIDITY = .0435
RAMJETS #26 & #27 [MOD. EXIT #2]
ROTOR ANGLE = 33°

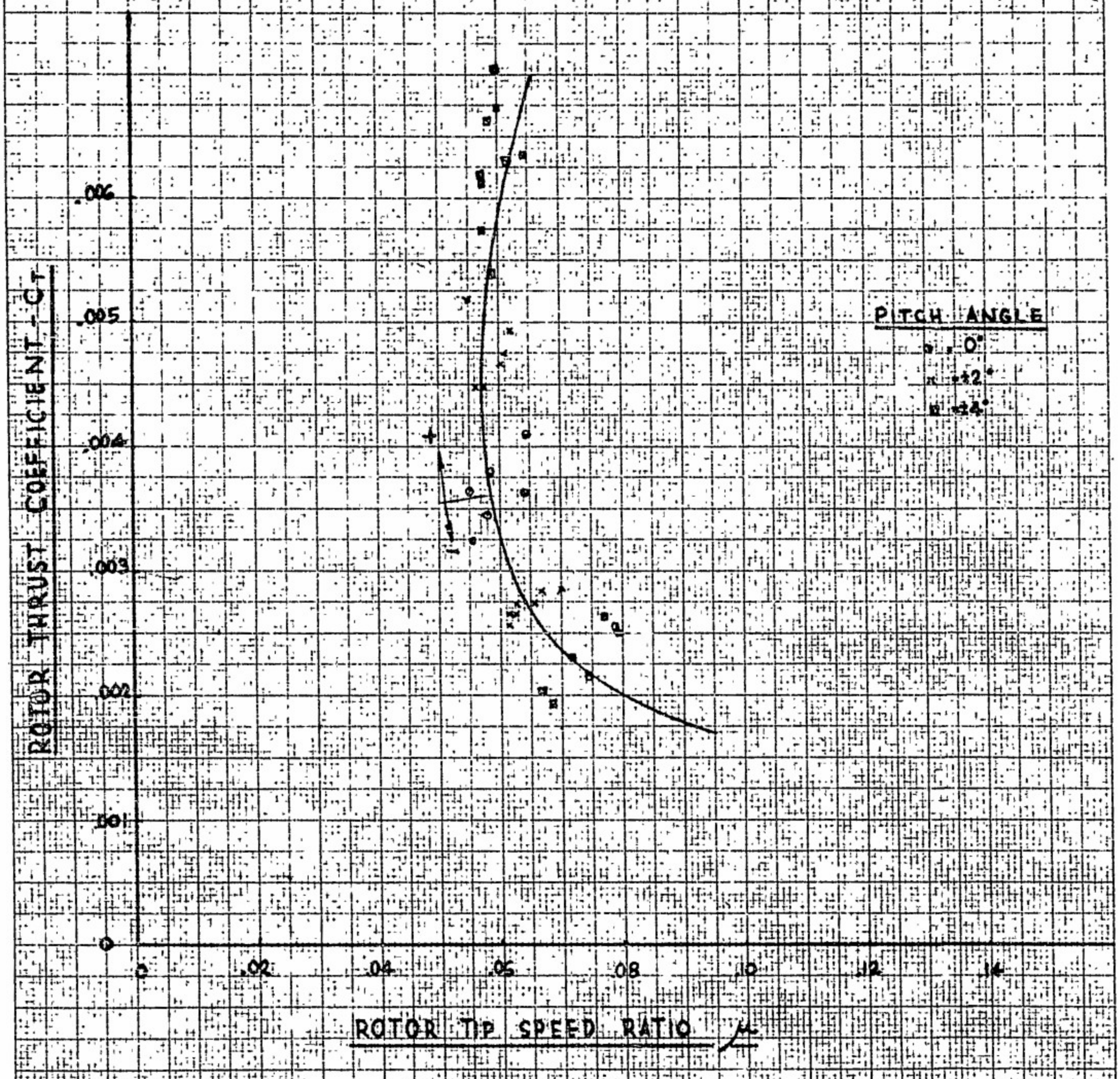

FIGURE 16

MODEL XH-20 ROTOR AND RAMJETS

VARIATION OF ROTOR THRUST COEFFICIENT WITH TIP SPEED RATIO & ROTOR ANGLE

ROTOR DIA. = 20 FT.
ROTOR SOLIDITY = .0435
RAMJETS #26 & #27 (MOD. EXIT #2)

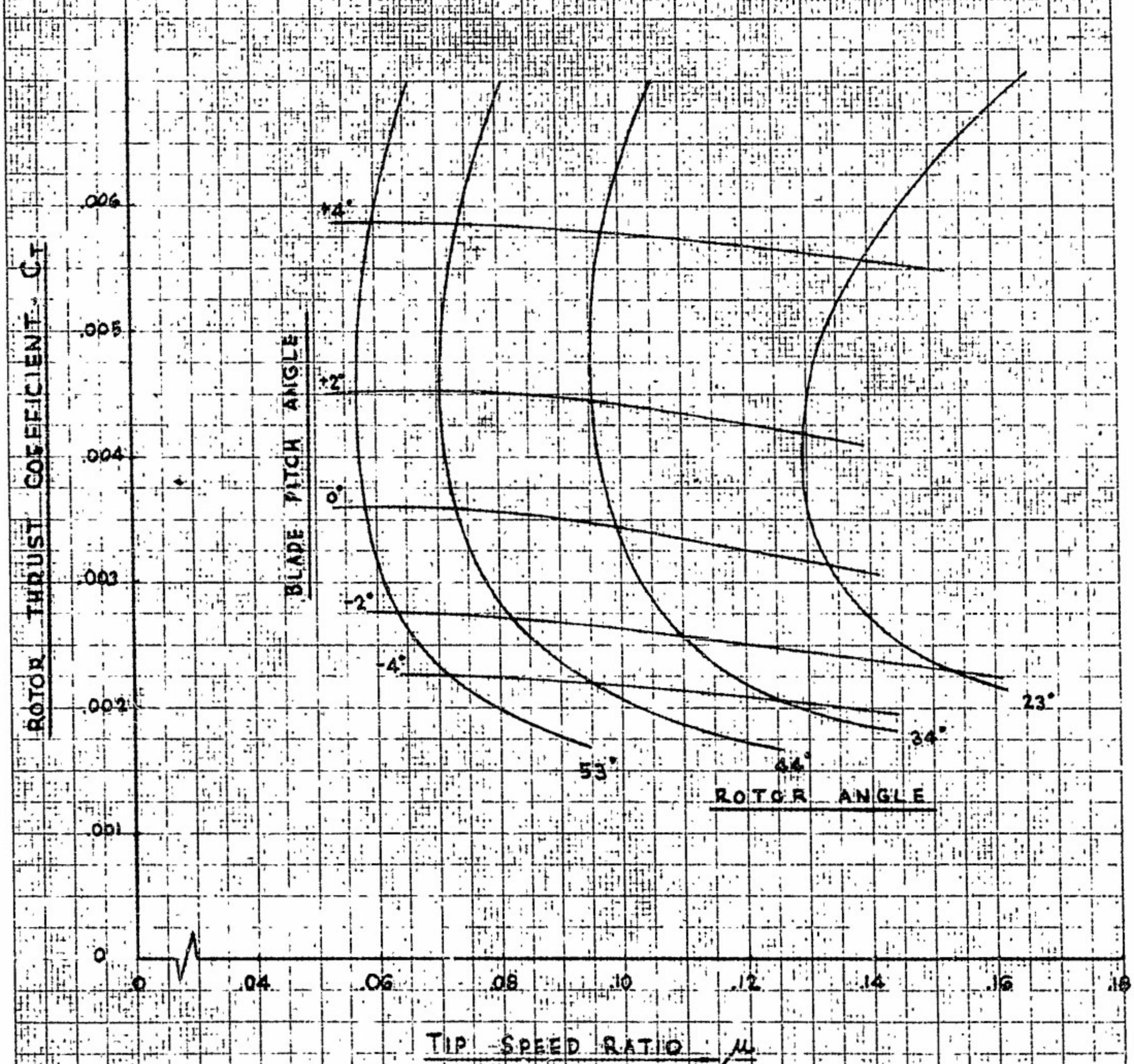

TABLE 3
Theoretical Dimensional Plot for Rate of Descent
Gross Weight = 550 pounds
Rotor Diameter = 20 feet
Rotor Solidity = .0435
Ram Jet C_{D_J} = .000122

μ	ΩR	350	400	450	500
	C_T	.00601	.00461	.00364	.00295
	C_T/σ	.139	.106	.084	.0678
.10	$\left(\frac{D}{L}\right)_R$	.440	.370	.335	.323
	$2\left(\frac{D}{L}\right)_J$	.206	.270	.334	.424
	$\tan \gamma$	.646	.640	.669	.757
.15	$\left(\frac{D}{L}\right)_R$	.230	.198	.186	.188
	$2\left(\frac{D}{L}\right)_J$	.140	.182	.224	.287
	$\tan \gamma$	.370	.380	.410	.475
.20	$\left(\frac{D}{L}\right)_R$	.151	.136	.130	.135
	$2\left(\frac{D}{L}\right)_J$	.108	.140	.173	.220
	$\tan \gamma$	.259	.276	.303	.355
.25	$\left(\frac{D}{L}\right)_R$	.111	.103	.101	.105
	$2\left(\frac{D}{L}\right)_J$	.088	.116	.144	.184
	$\tan \gamma$	.199	.219	.245	.289
.10	V_H	35	40	45	50
	V_V	22.6	25.6	30.1	37.9
.15	V_H	52.5	60	67.5	75.
	V_V	19.4	22.8	27.7	35.6
.20	V_H	70	80	90	100
	V_V	18.1	22.1	27.3	35.5
.25	V_H	87.5	100	112.5	125
	V_V	17.4	21.9	27.6	36.1

TABLE 4
Test Dimensional Plot for Rate of Descent
Gross Weight = 550 pounds
Rotor Dia. = 20 feet
Rotor Solid. = .0435
Ram Jets #26 and #27 with modified exit #2

γ	ΩR	350	400	450	500
	C_T	.00601	.00461	.00364	.00295
23°	μ	.145	.1305	.1298	.136
	V_h	50.6	52.1	58.4	68.0
	V_v	21.5	22.1	24.8	28.9
34°	μ	.0982	.0955	.098	.104
	V_h	34.4	38.2	44.1	52.0
	V_v	23.2	25.8	29.7	35.1
44°	μ	.0745	.0705	.0725	.0785
	V_h	26.1	28.2	32.6	39.2
	V_v	25.2	27.2	31.5	37.8
53°	μ	.060	.057	.058	.0615
	V_h	21.0	22.8	26.1	30.7
	V_v	27.9	30.2	34.6	40.8

FIGURE 17

MODEL XH-20 ROTOR AND RAMJETS

VARIATION OF RATE OF DESCENT WITH HORIZONTAL VELOCITY AND TIP SPEED

ROTOR DIA. = 20 FT.

ROTOR SOLIDITY = .0435

RAMJETS #26 & #27 [MOD. EXIT #2]

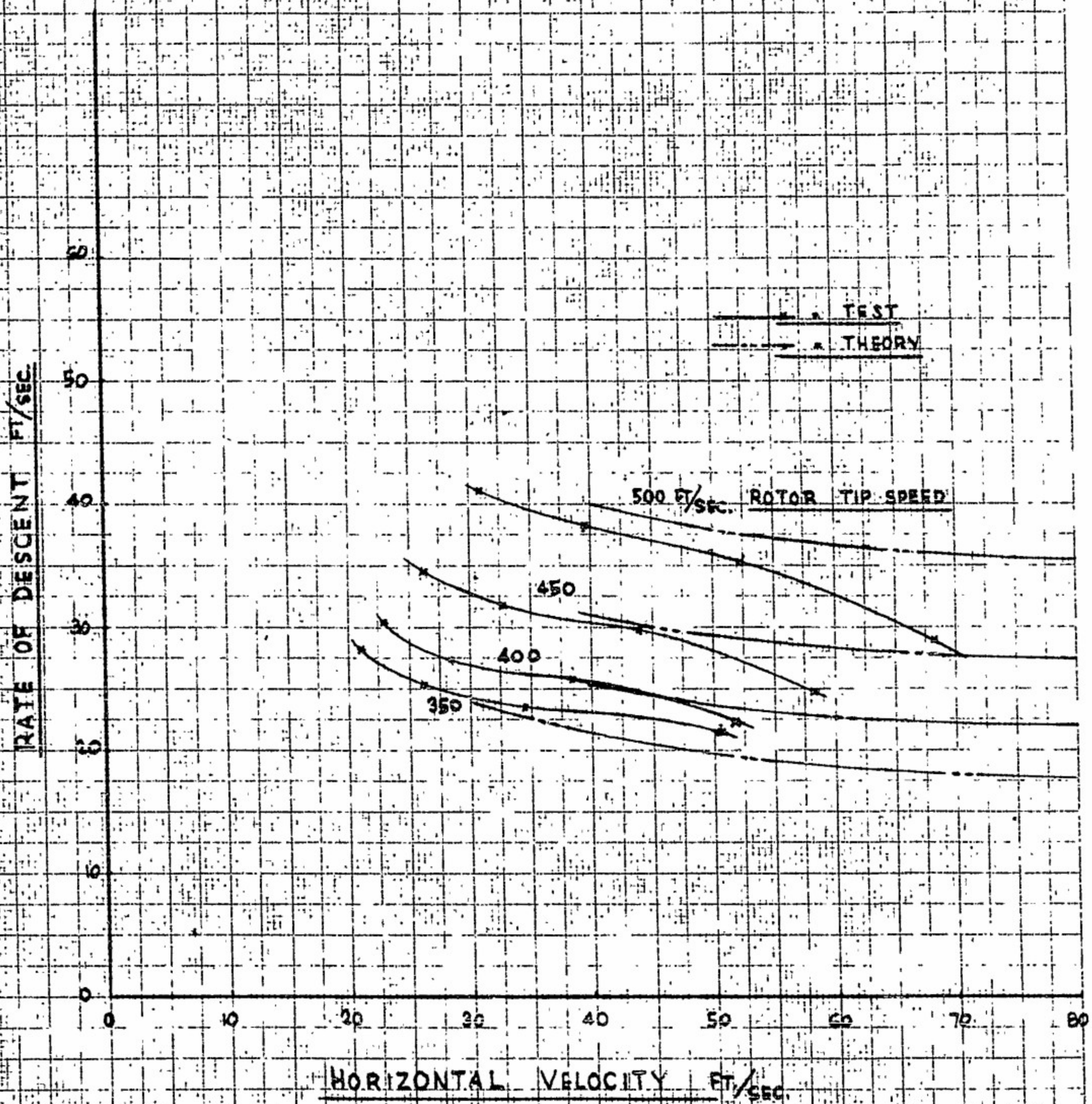

FIGURE 18

MODEL XH-38 ROTOR AND RAMJETS

VARIATION OF ROTOR THRUST COEFFICIENT
WITH TIP SPEED RATIO FOR
ROTOR DIA. = 20 FT.
ROTOR SOLIDITY = .0531
RAMJETS #26 & #27 [MOD EXIT #2]
ROTOR ANGLE = 2½°

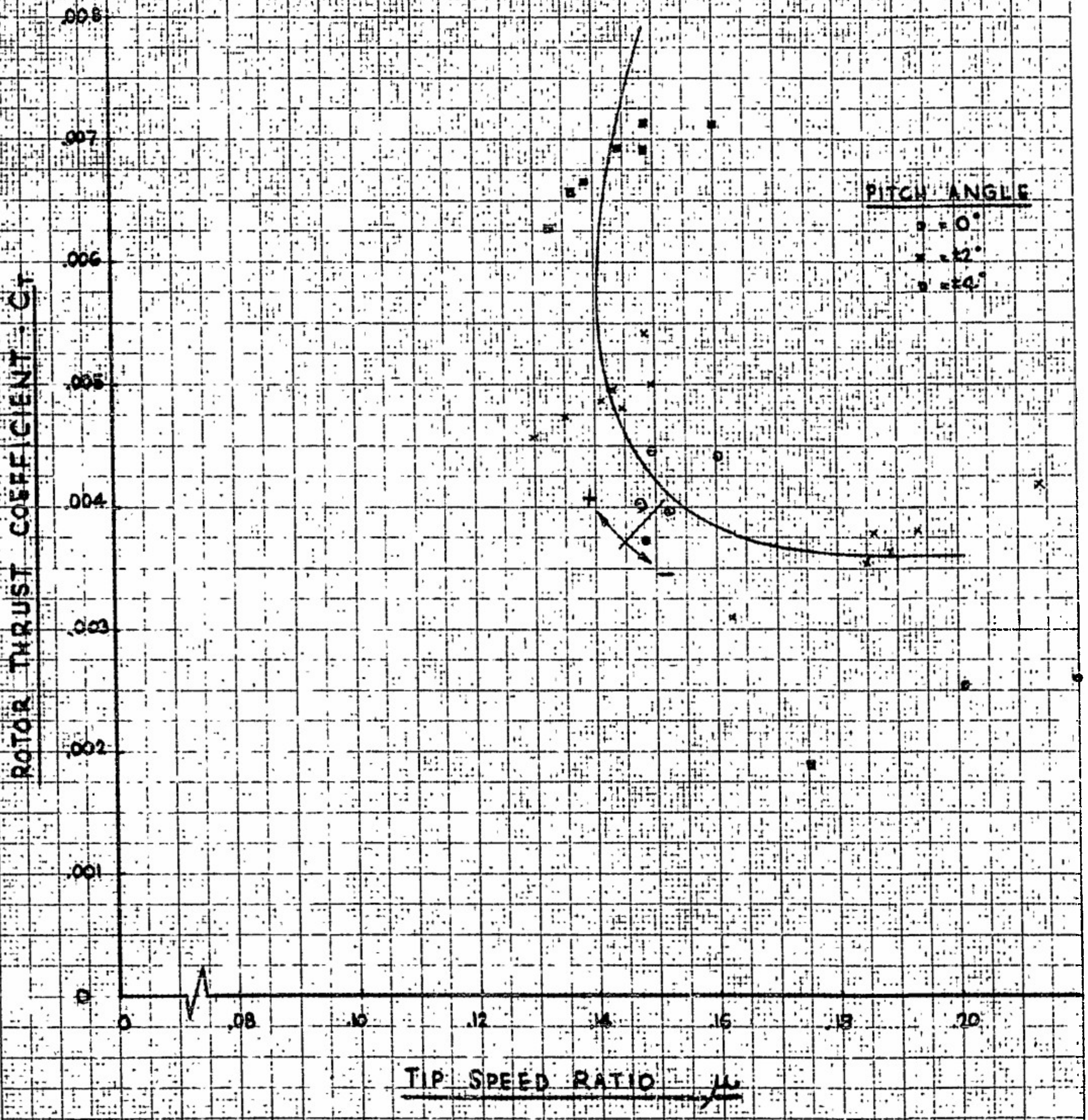

FIGURE 12

MODEL [illegible] ROTOR AND RAMJETS

VARIATION OF ROTOR THRUST COEFFICIENT
WITH TIP SPEED RATIO FOR
ROTOR DIA. = 20 FT.
ROTOR SOLIDITY = .0531
RAMJETS #26 & #27 [MOD. EXIT #2]
ROTOR ANGLE = 34°

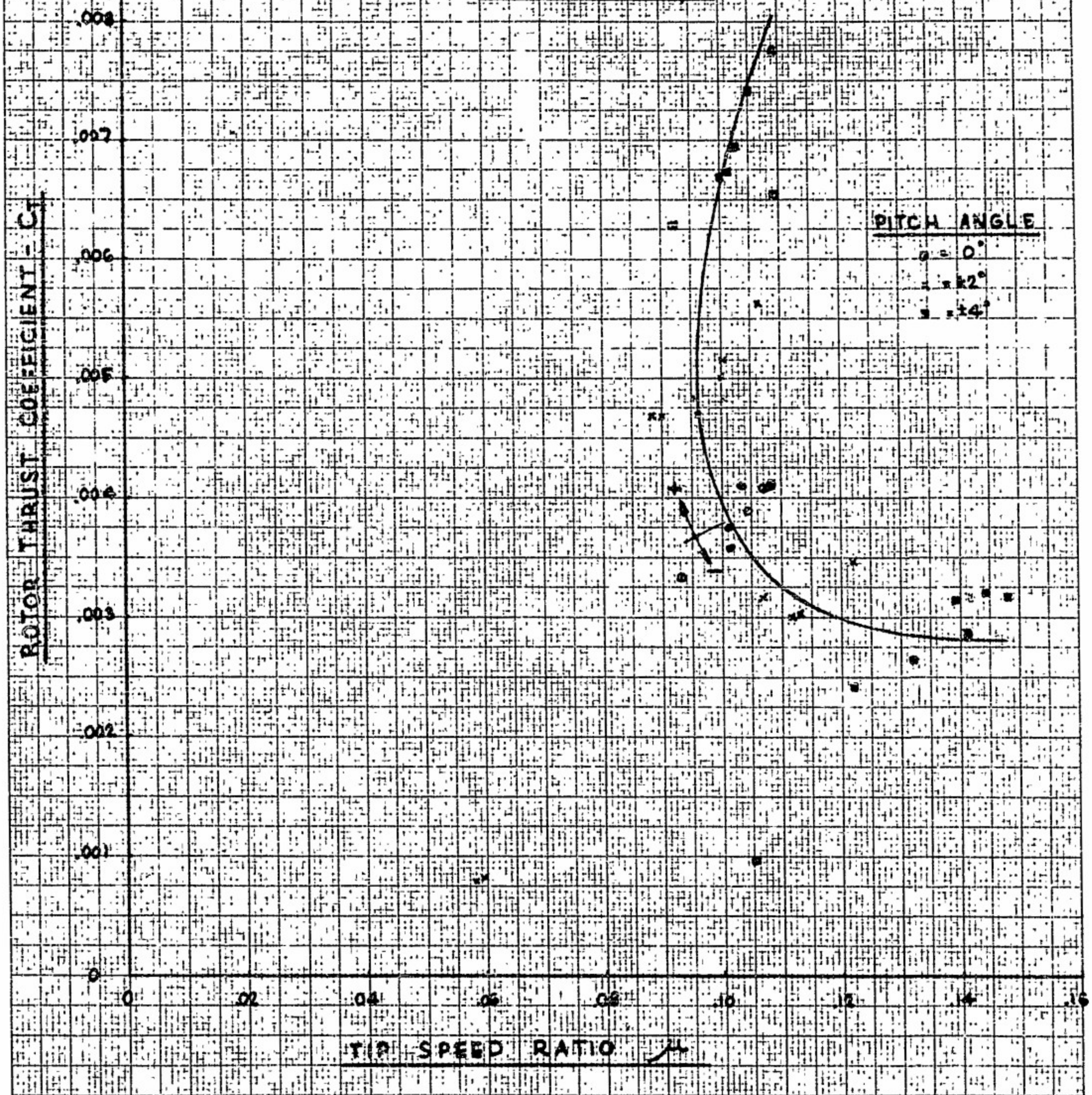

FIGURE 20

MODEL XH-20 ROTOR AND RAMJETS

VARIATION OF ROTOR THRUST COEFFICIENT
WITH TIP SPEED RATIO FOR
ROTOR DIA. = 20 FT.
ROTOR SOLIDITY = .0531
RAMJETS #26 & #27 (MOD. EXIT #2)
ROTOR ANGLE = 44°

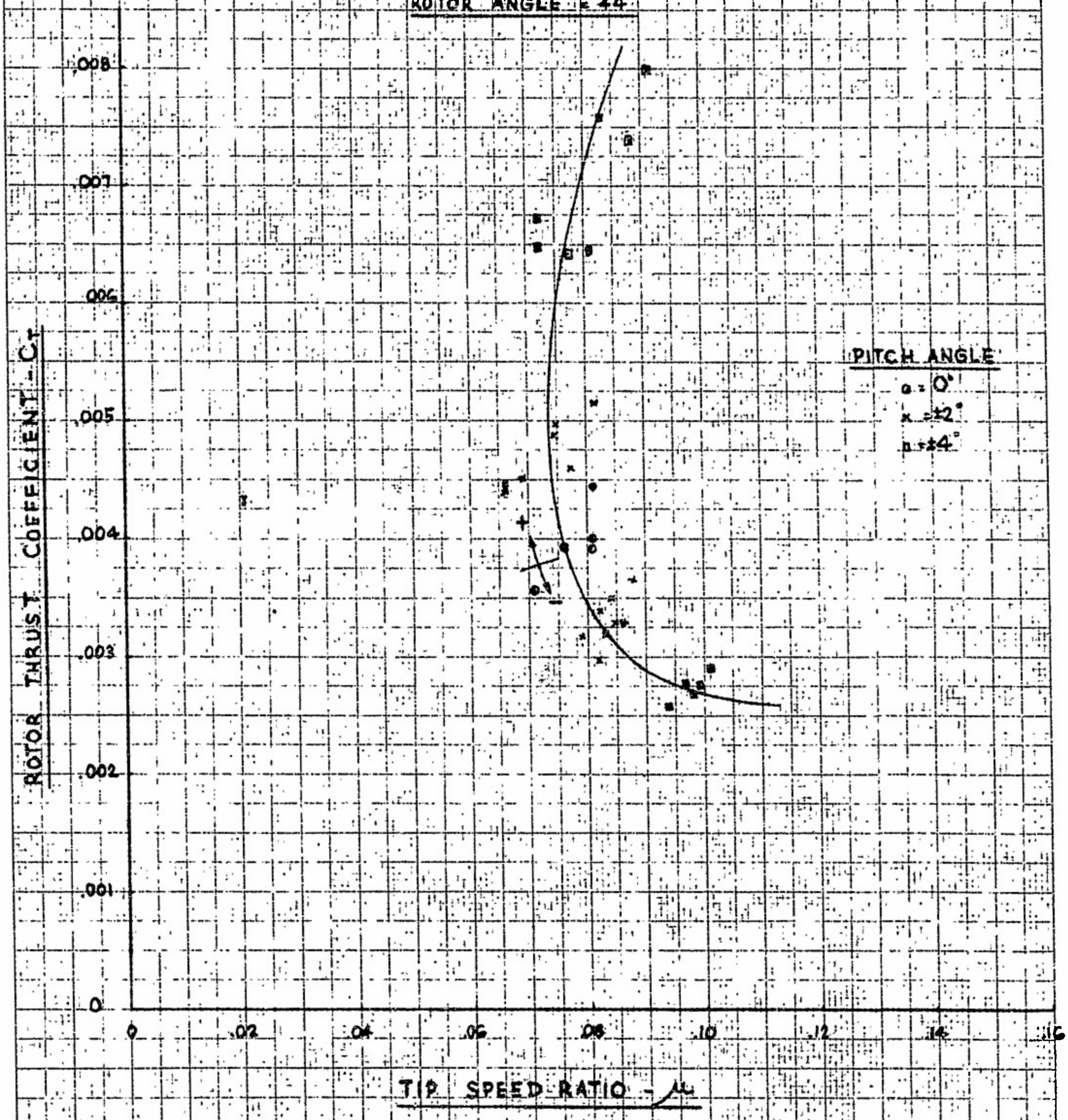

FIGURE 21

MODEL XH-20 ROTOR AND RAMJETS

VARIATION OF ROTOR THRUST COEFFICIENT
WITH TIP SPEED RATIO FOR
ROTOR DIA. = 20 FT.
ROTOR SOLIDITY = .0531
RAMJETS #26 & #27 [MOD. EXIT #2]
ROTOR ANGLE = 53°

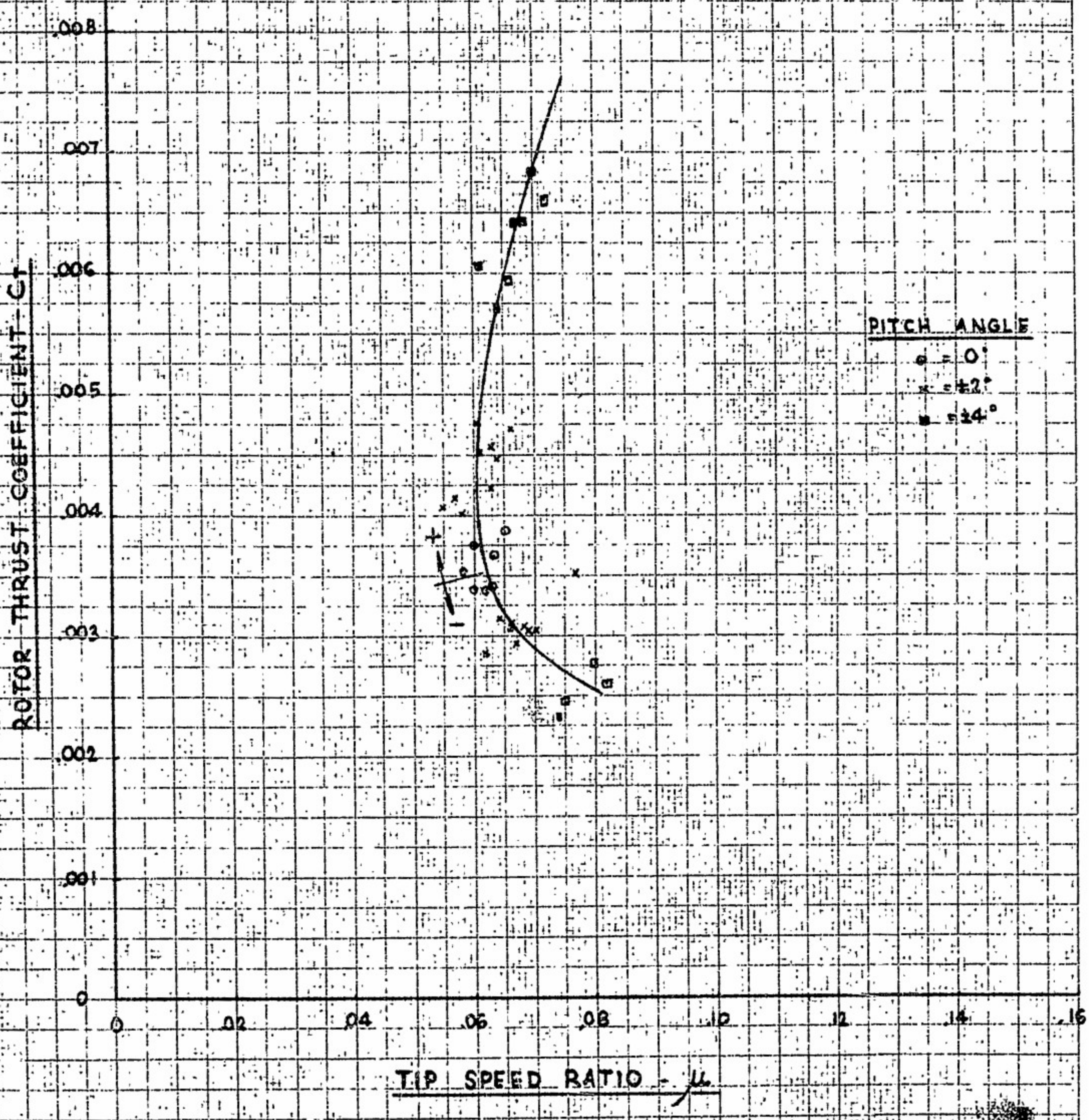

TABLE 5

Test Dimensional Plot for Rate of Descent

Gross Weight = 550 pounds
Rotor Diameter = 20 feet
Rotor Solidity = 0531
Ram Jets #26 and #27 (Mod. exit #2)

γ	ΩR	350	400	450	500
	C_T	.00601	.00461	.00364	.00295
23°	μ	.141	.152	.17	
	V_h	49.3	60.7	76.4	
	V_v	20.9	25.8	32.4	
34°	μ	.098	.0972	.1038	.123
	V_h	34.3	38.9	46.6	61.5
	V_v	23.1	26.2	31.4	41.5
44°	μ	.073	.074	.078	.089
	V_h	26.2	29.6	35.1	44.5
	V_v	25.3	28.6	33.9	43.0
53°	μ	.0646	.0608	.0615	.0685
	V_h	22.6	24.3	27.7	34.2
	V_v	30.0	32.2	36.8	46.4

TABLE 6

Theoretical Dimensional Plot for Rate of Descent

Gross Weight = 550 pounds

Rotor Diameter = 20 feet

Rotor Solidity = .0531

Ram jet C_{D_J} = .000122

μ	ΩR	350	400	450	500
	C_T	.00601	.00461	.00364	.00295
	C_T/σ	.1132	.0868	.0704	.0555
.10	$\left[\frac{D}{L}\right]_R$	.435	.382	.356	348
	$2\left[\frac{D}{L}\right]_J$	2(.104)	2(.136)	2(.163)	2(.214)
	$\tan\gamma$	.643	.654	.682	.776
.15	$\left[\frac{D}{L}\right]_R$	.230	.210	.205	.210
	$2\left[\frac{D}{L}\right]_J$	2(.070)	2(.092)	2(.114)	2(.143)
	$\tan\gamma$	.370	.394	.433	.496
.20	$\left[\frac{D}{L}\right]_R$	.153	.140	.142	.152
	$2\left[\frac{D}{L}\right]_J$	2(.054)	2(.071)	2(.086)	2(.112)
	$\tan\gamma$	.261	.282	.314	.376
.25	$\left[\frac{D}{L}\right]_R$	.112	.108	.110	.118
	$2\left[\frac{D}{L}\right]_J$	2(.044)	2(.059)	2(.083)	2(.092)
	$\tan\gamma$	.200	.226	.276	.302
.10	V_H	35	40	45	50
	V_V	22.5	26.2	30.7	38.8
.15	V_H	52.5	60	67.5	75
	V_V	19.4	23.7	29.2	37.2
.20	V_H	70	80	90	100
	V_V	18.25	22.6	28.3	37.6
.25	V_H	87.5	100	112.5	125
	V_V	17.5	22.6	31.1	37.8

FIGURE 22

MODEL XH-20 ROTOR AND RAMJETS

VARIATION OF ROTOR THRUST COEFFICIENT WITH TIP SPEED RATIO AND ROTOR ANGLE

ROTOR DIA. = 20 FT.

ROTOR SOLIDITY = .0531

RAMJETS #26 & #27 [MOD. EXIT #2]

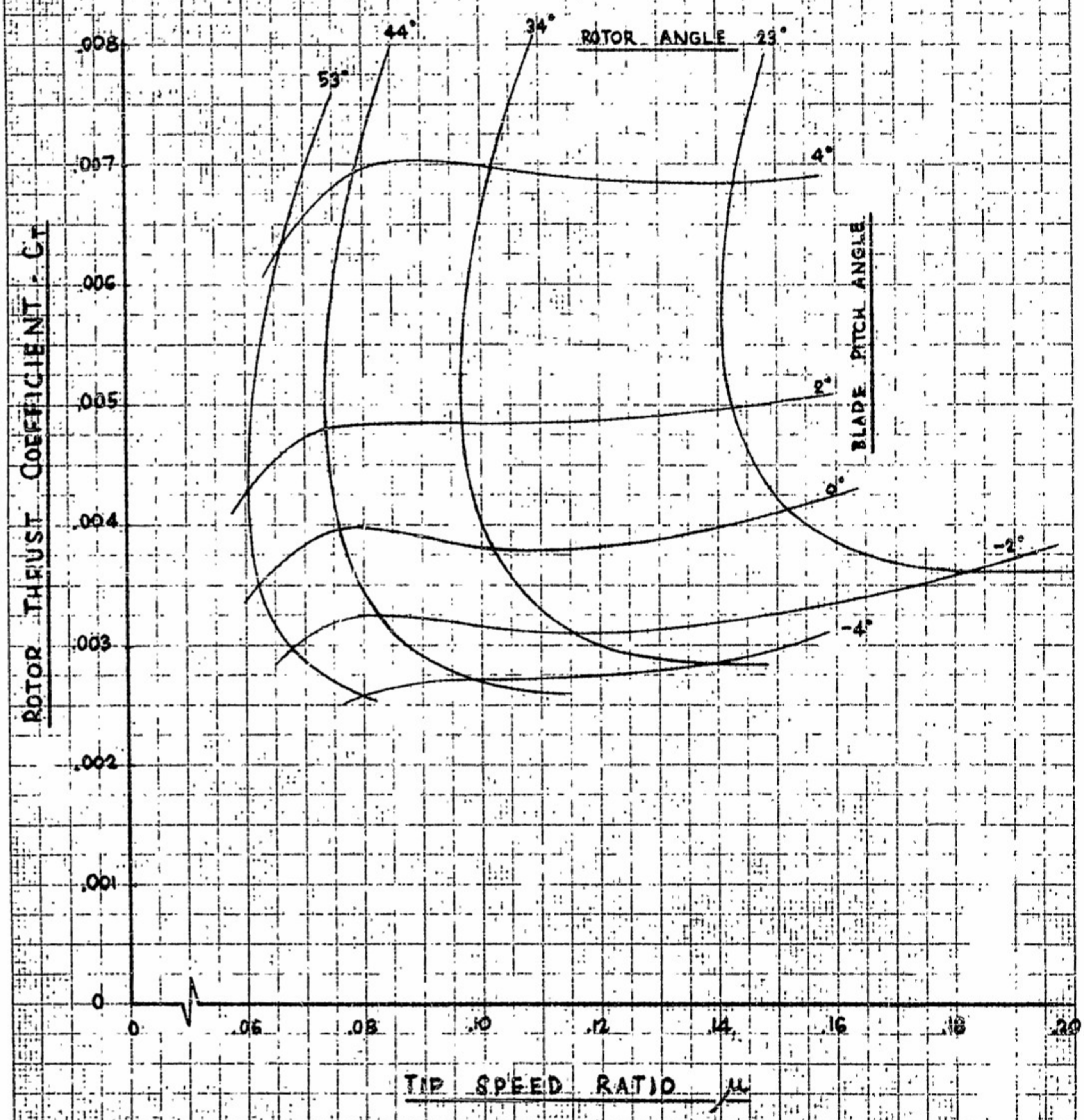

FIGURE 23

MODEL XH-20 ROTOR AND RAMJETS

VARIATION OF RATE OF DESCENT WITH HORIZONTAL VELOCITY AND TIP SPEED

ROTOR DIA. = 20 FT.
ROTOR SOLIDITY = .0531
RAMJETS #26 & #27 [MOD. EXIT #2]
RAMJET DRAG COEFFICIENT = .000122

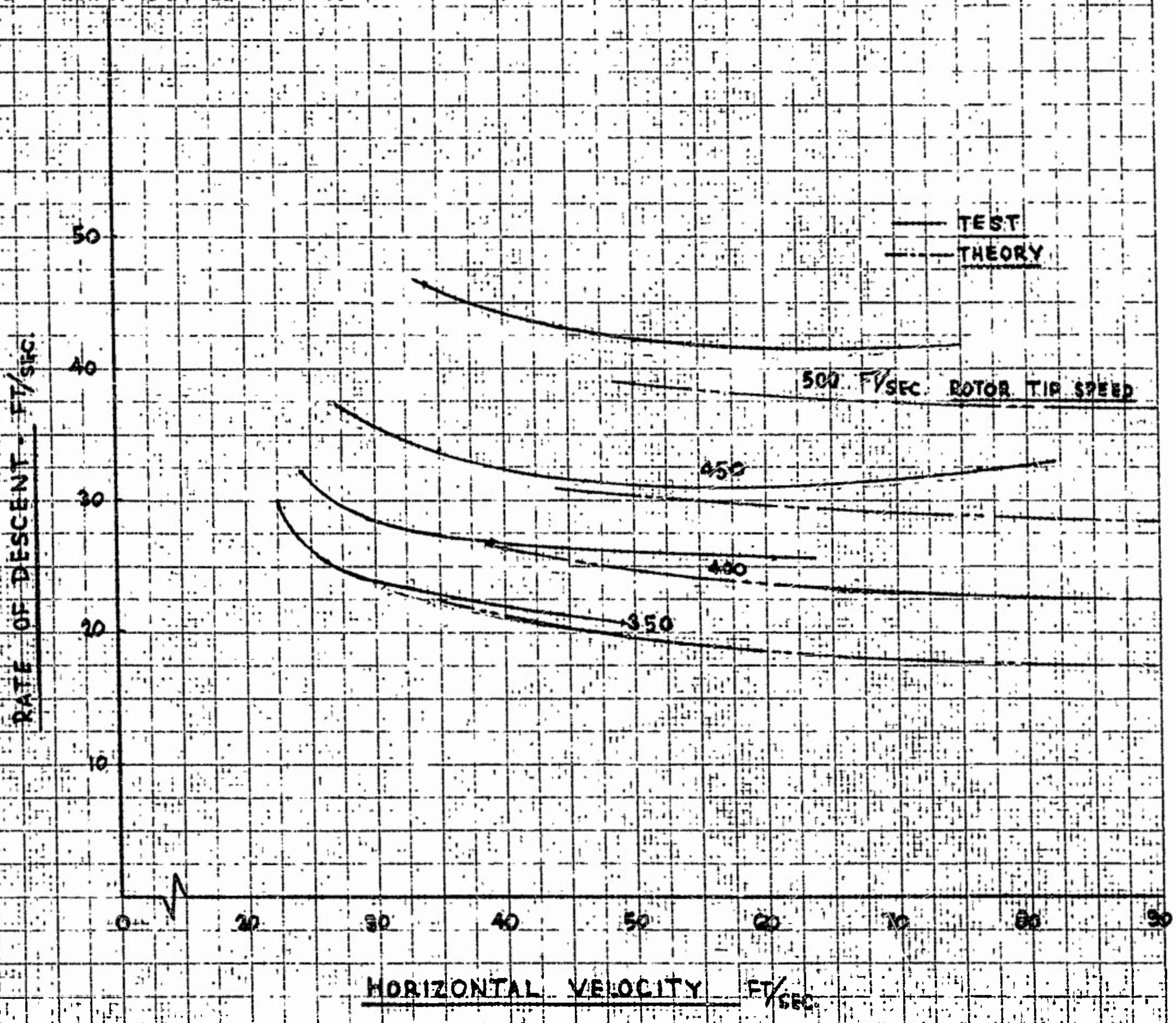

FIGURE 24

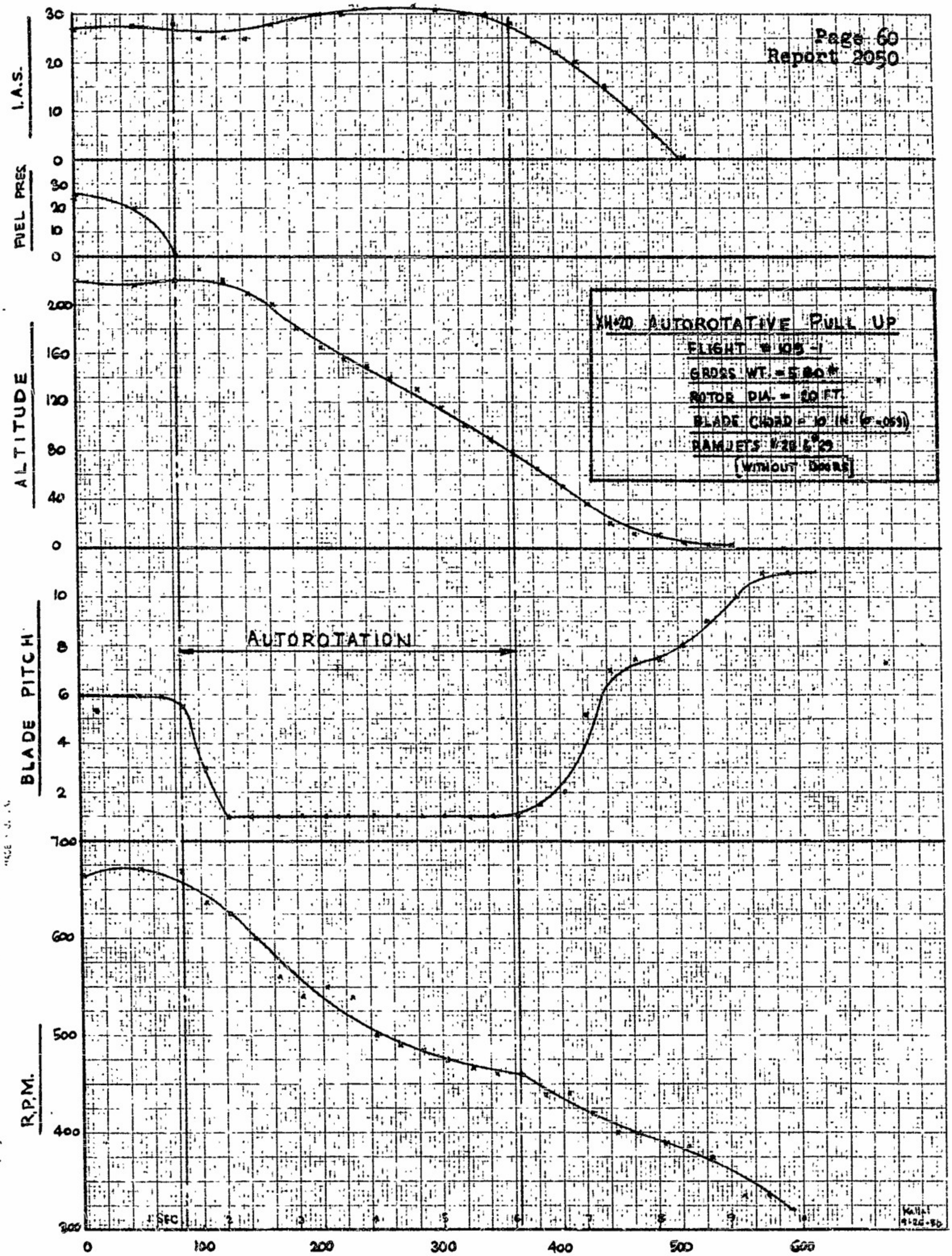
I.A.S.
FUEL PRES
ALTITUDE
BLADE PITCH
R.P.M.
AUTOROTATION
XH-20 AUTOROTATIVE PULL UP
FLIGHT # 105-1
GROSS WT. = 580#
ROTOR DIA. = 20 FT.
BLADE CHORD = 10 IN.
RAMJETS #28 & 29
(WITHOUT DOORS)
SEC
0
100
200
300
400
500
600

FIGURE 25

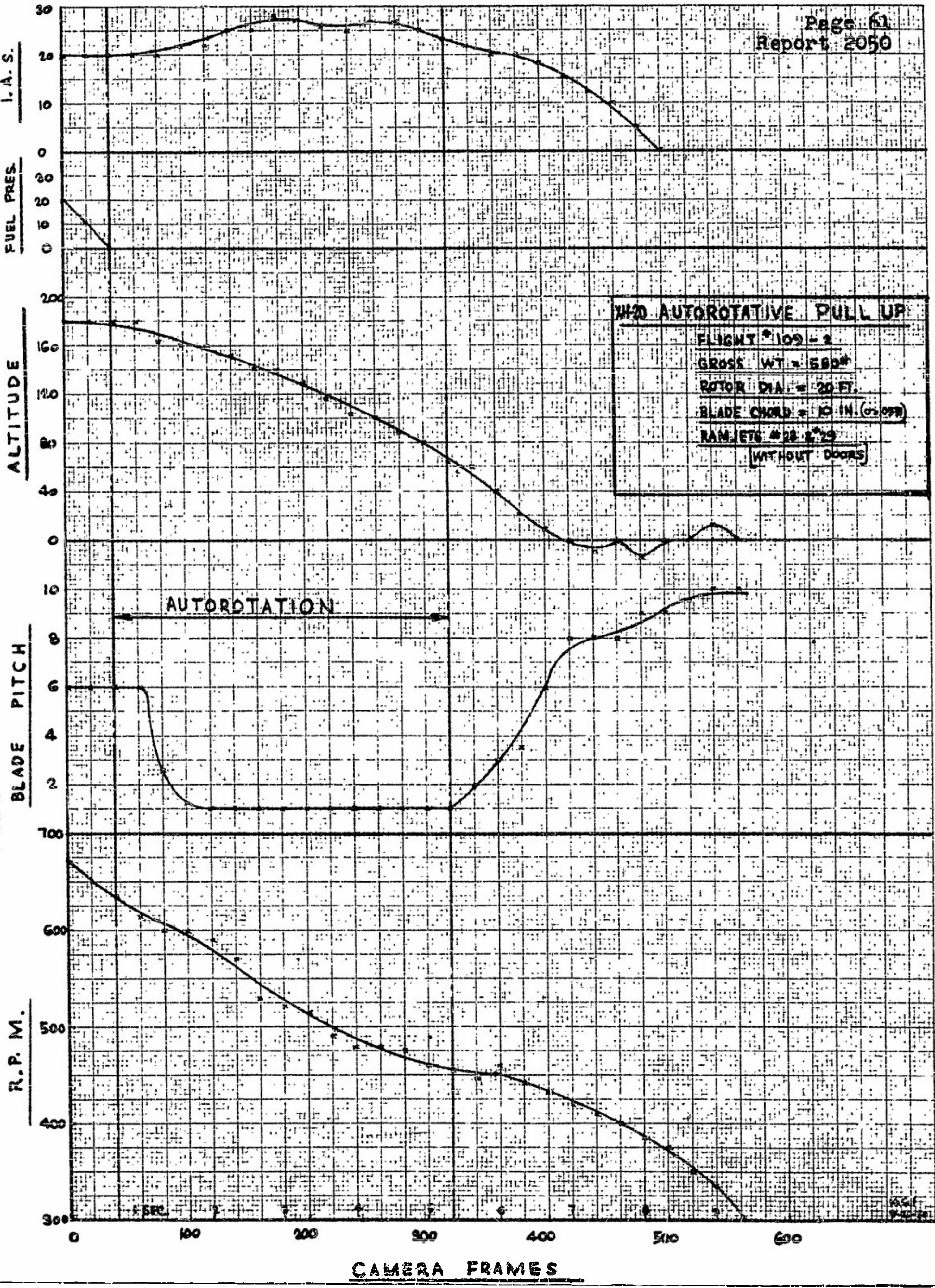
I. A. S.
FUEL PRES.
ALTITUDE
BLADE PITCH
R. P. M.
AUTOROTATION
XH-20 AUTOROTATIVE PULL UP
FLIGHT # 109 - 2
GROSS WT = 580#
ROTOR DIA. = 20 FT.
BLADE CHORD = 10 IN.
RAMJETS #28 & #29
[WITHOUT DOORS]
0
100
200
300
400
500
600
CAMERA FRAMES

FIGURE 26

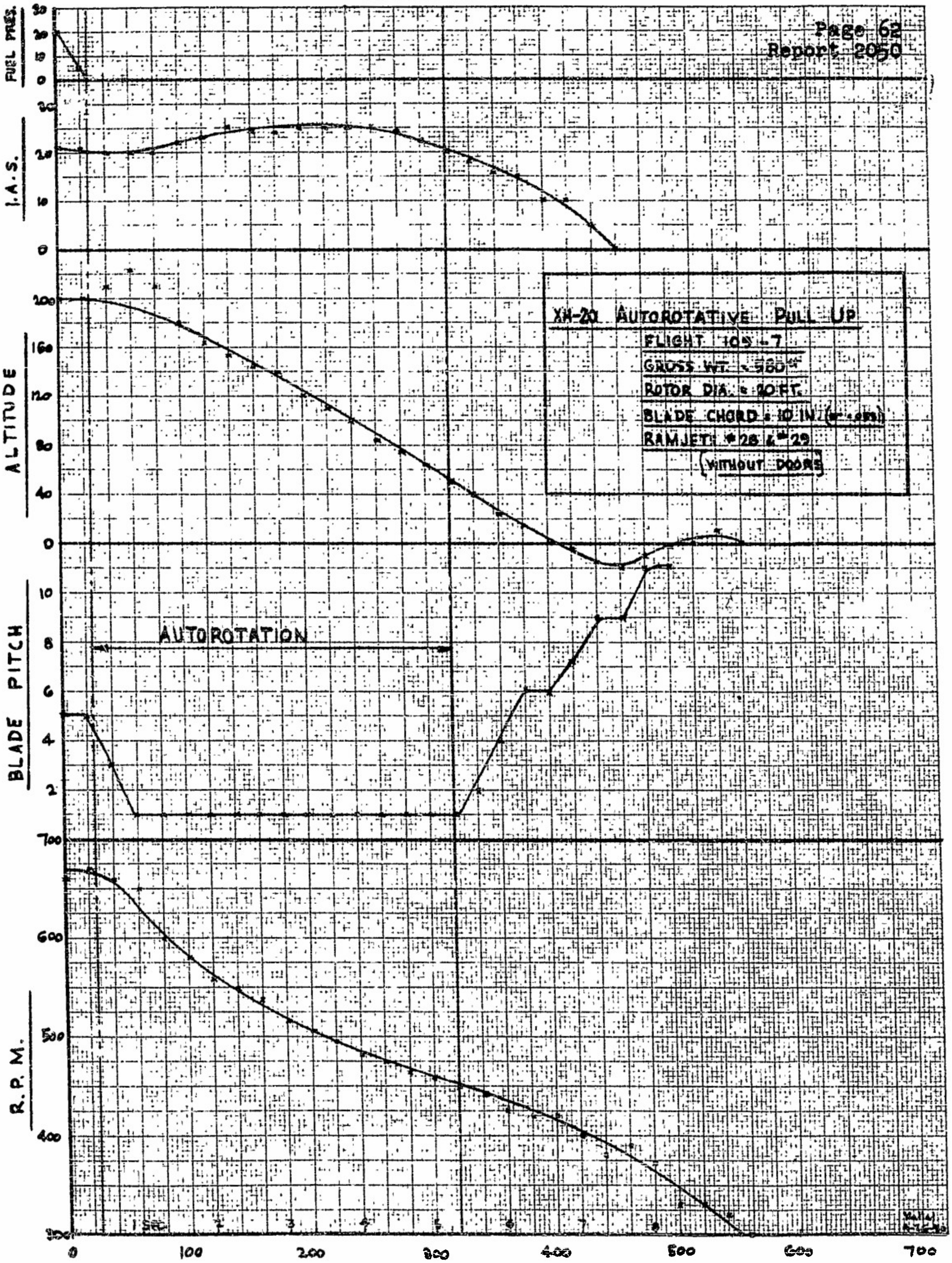
FUEL PRES.
I.A.S.
ALTITUDE
BLADE PITCH
R.P.M.
XH-20 AUTOROTATIVE PULL UP
FLIGHT 105-7
ROTOR DIA. = 20 FT.
AUTOROTATION
CAMERA FRAMES

FIGURE 27

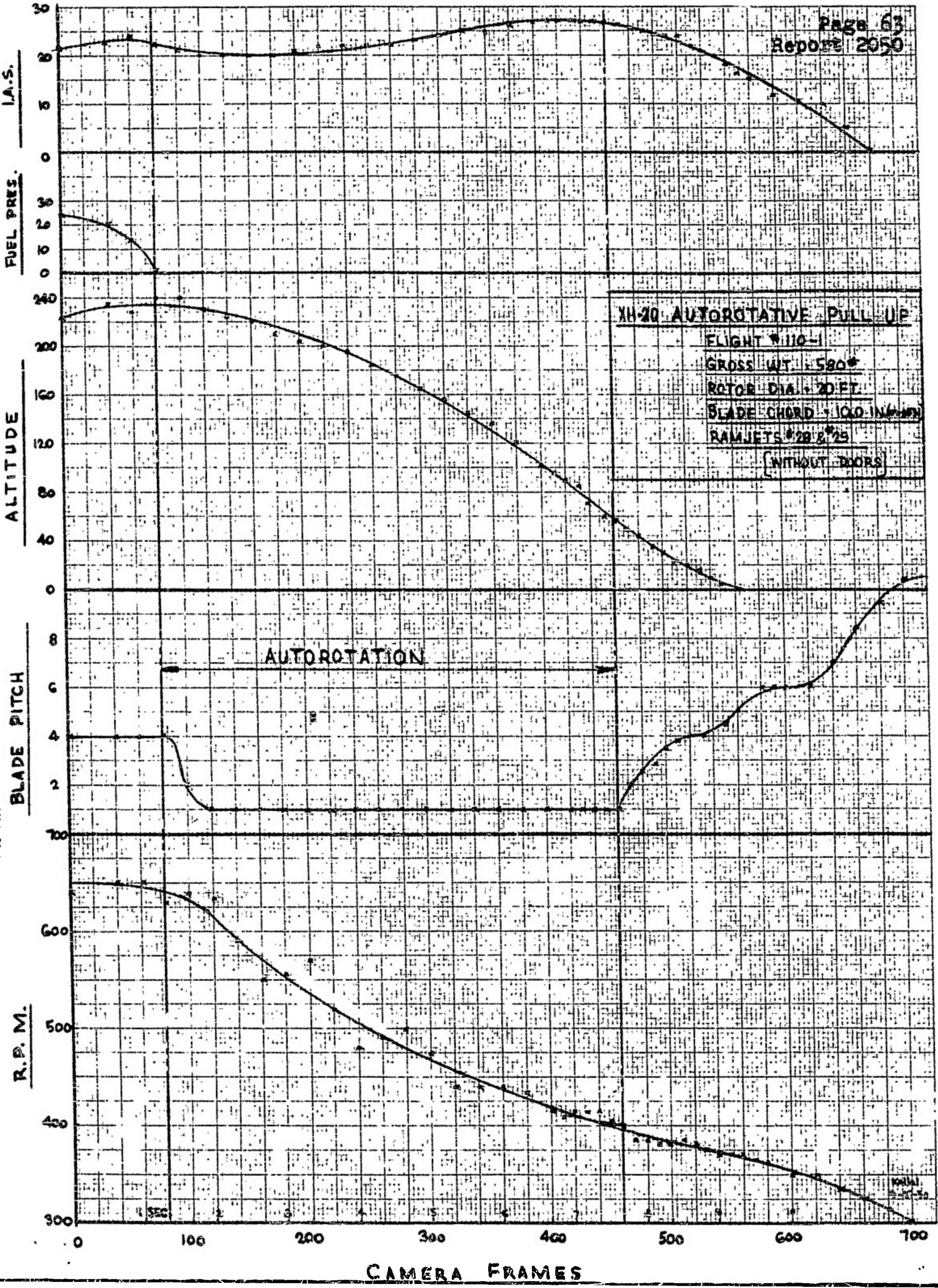
I.A.S.
FUEL PRES.
ALTITUDE
BLADE PITCH
R.P.M.
XH-20 AUTOROTATIVE PULL UP
FLIGHT # 110-1
GROSS WT. - 580#
ROTOR DIA. - 20 FT.
BLADE CHORD - 10.0 IN.
RAMJETS #28 & #29
(WITHOUT DOORS)
AUTOROTATION
1 SEC
CAMERA FRAMES
KEUFFEL & ESSER CO.

FIGURE 28

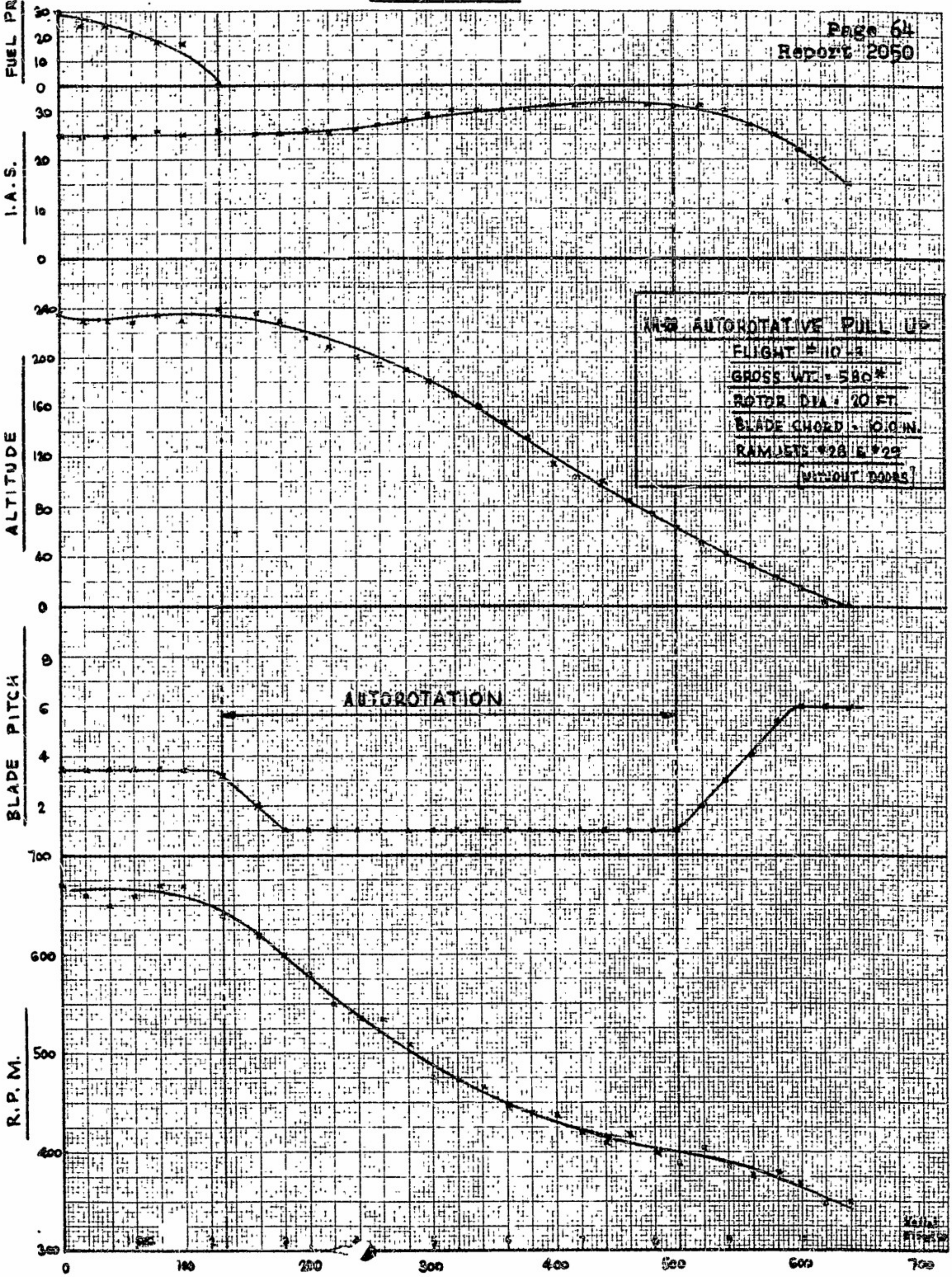
FUEL PR.
I.A.S.
ALTITUDE
BLADE PITCH
R.P.M.
AUTOROTATIVE PULL UP
FLIGHT #110-3
GROSS WT. = 580#
ROTOR DIA. = 20 FT.
BLADE CHORD = 10.0 IN.
RAMJETS #28 & #29
WITHOUT DOORS
AUTOROTATION
0
100
200
300
400
500
600
700

FIGURE 29

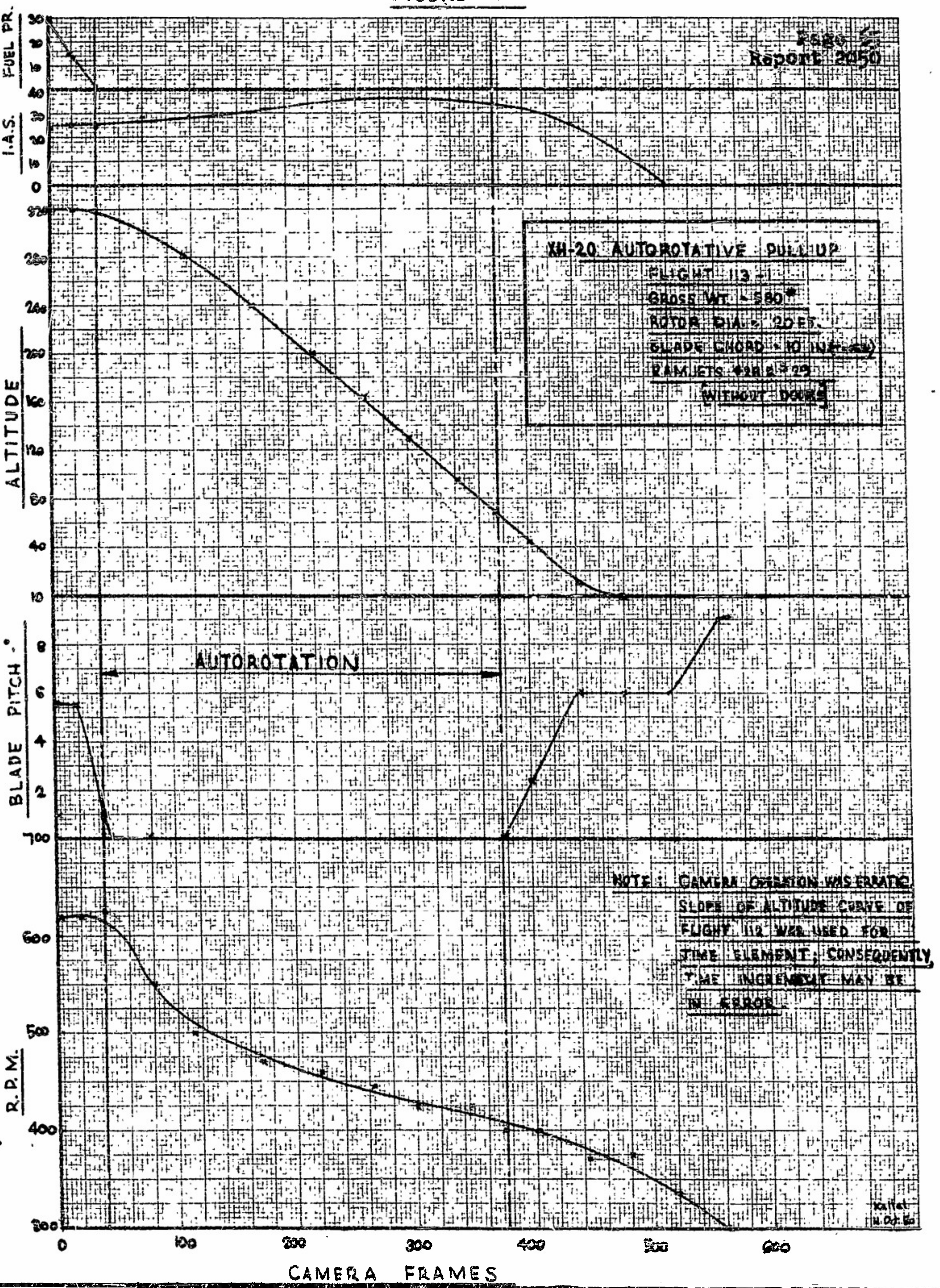

Report 2050
FUEL PR.
I.A.S.
ALTITUDE
BLADE PITCH °
R.P.M.
AUTOROTATION
XH-20 AUTOROTATIVE PULL UP
FLIGHT 113-1
GROSS WT. - 580#
ROTOR DIA. = 20 FT.
BLADE CHORD = 10 IN.
RAMJETS #28 & #29
(WITHOUT DOORS)
NOTE: CAMERA OPERATION WAS ERRATIC.
SLOPE OF ALTITUDE CURVE OF
FLIGHT 112 WAS USED FOR
TIME ELEMENT; CONSEQUENTLY,
TIME INCREMENT MAY BE
IN ERROR.
CAMERA FRAMES

FIGURE 30

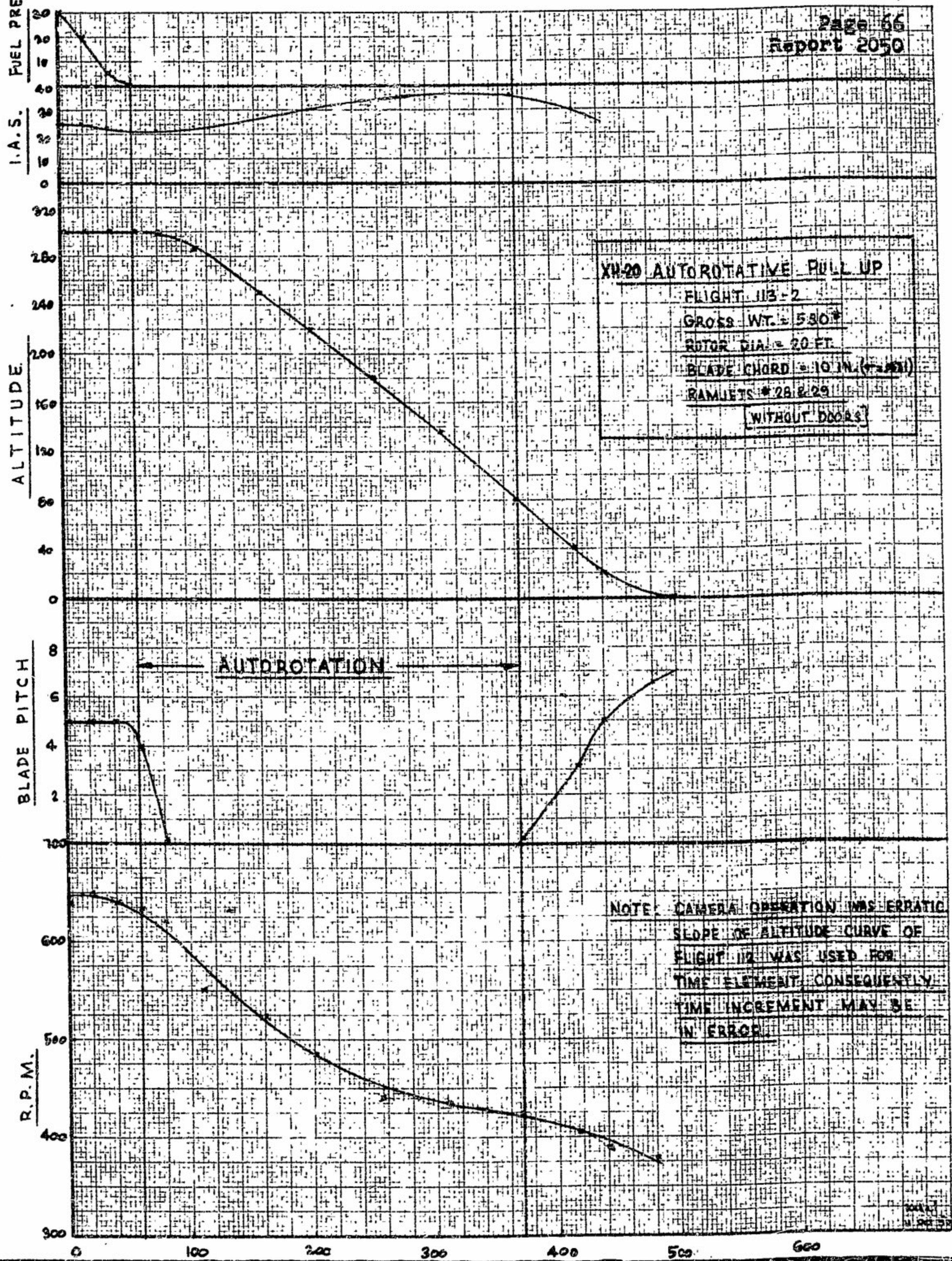
FUEL PRES.
I.A.S.
ALTITUDE
BLADE PITCH
R.P.M.
AUTOROTATION
XH-20 AUTOROTATIVE PULL UP
FLIGHT 113-2
GROSS WT. = 550#
ROTOR DIA. = 20 FT.
BLADE CHORD = 10 IN.
RAMJETS # 28 & 29
WITHOUT DOORS
NOTE: CAMERA OPERATION WAS ERRATIC
SLOPE OF ALTITUDE CURVE OF
FLIGHT 112 WAS USED FOR
TIME ELEMENT. CONSEQUENTLY
TIME INCREMENT MAY BE
IN ERROR.
0
100
200
300
400
500
600